8-9-2014

DESIGN, SYNTHESIS, CHARACTERIZATION, AND EVALUATION OF SURFACE MODIFIED BORONATE ESTER COVALENT ORGANIC FRAMEWORKS

Matthew W. Di Carmine
University of South Carolina - Columbia

DESIGN, SYNTHESIS, CHARACTERIZATION, AND EVALUATION OF SURFACE MODIFIED BORONATE ESTER COVALENT ORGANIC FRAMEWORKS

by

Matthew W. Di Carmine

Bachelor of Science
Quinnipiac University, 2010

Submitted in Partial Fulfillment of the Requirements

For the Degree of Master of Science in

Chemistry

College of Arts and Sciences

University of South Carolina

2014

Accepted by:

John J. Lavigne, Director of Thesis

Perry J. Pellechia, Reader

Lacy Ford, Vice Provost and Dean of Graduate Studies

Dedication

This work is dedicated to St. Jude.

Acknowledgements

I would like to start off by thanking my family, especially my parents for helping me every step of the way from childhood to adulthood and for always being there for me. Next, my sisters Kristen and Elisabeth, I'm excited to be 725 miles closer to you. Although, I may have missed several family vacations, the best is yet to come. To all of my New York friends, thanks for coming down to South Ca., and visiting, so glad it will only be a 7 minute drive to see you guys, compared to a 7 hour flight.

To all of the graduate students at the University of South Carolina for all your help along the way, especially: Tony, Perry, Mike, Jeff, Kayley, Atri, Anand, Ping, Robert, Alex, Cliff and Ravish. To past and to present group members thanks for teaching me how to be a better orator. Steven A. Sloope, thanks for contributing to this thesis and for running all of those UV-Vis for me. Lastly, thank you Dr. Perry Pellechia for your guidance, making time to run my samples, and reading my thesis.

Abstract

Covalent Organic Frameworks (COFs) were first reported in 2005 and are analogous to Metal Organic Frameworks (MOFs), with proposed applications in separation, storage and sequestration. Since COFs are comprised of lighter elements they are considered more advantageous for weight-sensitive applications. However, COFs are susceptible to degradation by weak nucleophiles such as water (i.e. hydrolysis). The Lavigne group has focused on developing structure-property relationships for COFs. It was previously demonstrated that the porosity of the COFs could be tailored by incorporating small alkyl chains on one monomer. Inclusion of these alkylated monomers into COF materials effectively increased the COF hydrophobicity resulting in materials with enhanced hydrolytic stability. However, the increased stability is accompanied by a decrease in pore size and subsequently, surface area. This work focused on maintaining the pore size, while increasing stability. This was achieved by attaching polymers to the surface of the framework. These modifications were made either by forming boronate esters on the surface edge of the COF, or by coordinating a polymer to the empty p-orbitals of boron on the surface face. We have found that incorporation of polymer into the framework results in increased COF stability.

Table of Contents

List of Tables

List of Figures

List of Abbreviations

AIBN ..... 2,2'-Azobis(2-methylpropionitrile

ATRP ..... Atom Transfer Radical Polymerization

BET ..... Brunauer-Emmett-Teller

BTBA ..... 1,3,5-Benzene triboronic acid

COF ..... Covalent Organic Framework

COF:P(4VP) ..... COF-18A:P(4VP) molar ratio

CP MAS ..... Cross polarization magic angle spinning

CRP ..... Controlled radical polymerization

CTA ..... Chain transfer agent

DCM ..... Methylene chloride

DSC ..... Differential scanning calorimetry

EDS ..... Energy-dispersive X-ray spectroscopy

MOF ..... Metal Organic Framework

NMR ..... Nuclear magnetic resonance

P(4VP) ..... Poly(4-Vinyl Pyridine)

PXRD ..... Powder X-Ray Diffraction

RAFT ..... Reversible addition Chain Transfer Fragmentation

T_g ..... Glass transition temperature

TGA ..... Thermogravimetric analysis

t-Plot ..... Thickness plot

THB ..... 1,2,4,5-Tetrahydroxy benzene

THF ..... Tetrahydrofuran

CHAPTER 1: Introduction

1.1 Overview

Microporous materials: zeolites, Metal Organic Frameworks (MOFs) and Covalent Organic Frameworks (COFs) are synthesized from a reticular synthesis, which requires multifunctional rigid building materials to form a predetermined frameworks[1,2]. The frameworks are then able to stack due to secondary building units. Unique properties of these materials are high surface area and high thermal stability.

1.2 Background

Metal organic frameworks (MOFs) have the potential utility for gas storage, separation, and purification. MOFs have the capability to bind to various host gases including hydrogen, carbon dioxide, methane and argon.[3,4]. In addition MOFs have surface area as high as 3200 m^2/g.[5]. Whereas MOFs are comprised of metals, COFs are comprised of lighter elements: boron, oxygen, and carbon. These lightweight materials offer the same potential utility, however, boron based COFs are susceptible to hydrolysis[6,7].

Boron is a hard Lewis acid, contains an empty *p*-orbital, and bonds reversibly with oxygen. The three main classes of boron compounds are shown in **Figure 1.1:** boronic acids, boronate esters or a triarm star anhydride (boroxine). Boronate ester

formation is unique since the chemical bond is covalent yet reversible. This reversibility deletes erroneous bonds and reforms the bonds correctly and covalently, thus allowing self-assembly to occur.

The Lavigne laboratory generally works with boronic acid and diol starting materials, which create boronate ester products, such as COF[8.9.10]. By using substituted THB monomers, COF-18Å and alkylated COF-18Å analogues were synthesized in a facile condensation polymerization. Results showed that having longer R groups on the THB monomer increases hydrolytic stability, but at the expense of microporosity. During this synthesis, excess THB monomer ensures the exterior of the COF is decorated with diols.

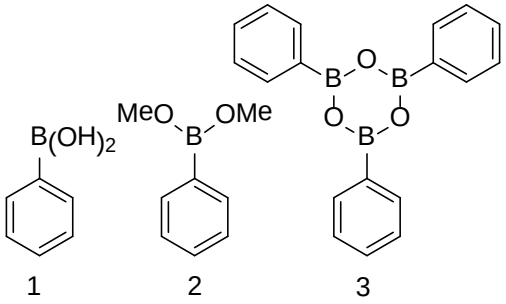

Figure 1.1
Types of boron compounds. **1)** boronic acid, **2)** boronate ester **3)** anhydride

Severin's group used a difunctional pyridine monomer to polymerize a trifunctional boronate ester with a monofunctional catechol[11]. The empty p-orbital allows for another compound that contains a lone pair of electrons to coordinate with boron as shown in **Figure 1.2**. Upon coordination, the hybridization of the boron species changes from sp^2 to sp^3, and this change in hybridization can also help to prevent hydrolysis, due

to the orbital on the boronate species now containing electrons. Several groups have investigated the structure property relationship of how incorporating a small pyridine molecule to COF-5, which was the fifth COF synthesized in Yaghi's group properties are impacted. These studies indicate that as the empty orbitals on the boronate component of COF become filled, an increase in stability is observed. However, the studies of macromolecular pyridine compounds incorporated on COF are in the nascent stages, and the results will be discussed in **Chapter 3** [12.13].

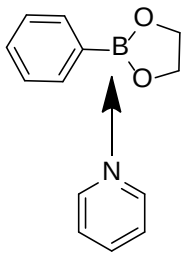

Figure 1.2

Nitrogen boron dative bond .Coordination of the lone pair of electrons on nitrogen to the empty p-orbitals on a boronate ester via a dative bond.

Atom Transfer Radical Polymerization (ATRP)[14] and Reversible Addition Chain Transfer Fragmentation polymerization (RAFT)[15]are two types of Controlled Radical Polymerizations (CRPs). Both CRP's rely on the persistent radical effect, for control of molecular weight, polydispersity (PDI), composition, and architecture. ATRP requires: nitrogen ligands, copper catalyst, monomer, and halogenated initiator. RAFT requires: an initiator (commonly AIBN 2,2'-Azobis(2-methylpropionitrile), a chain transfer agent (CTA), and a monomer. These are illustrated in **Figure 1.3**. RAFT generally allows for wider monomer choices without the use of a copper catalyst. The advantage is that the only change needed to transition from a free radical polymerization to RAFT is the

addition of a CTA. Previously, ATRP[16] and RAFT[17] incorporated boron into linear polymers on both the end group and the side chain. Jäkle and Sumerlin incorporated organoboron compounds into the side chain repeat unit using a derivatized styrene monomer, MBpin, shown in **Figure 1.3**. Jäkle[18] used ATRP technique whereas Sumerlin used a RAFT polymerization technique.

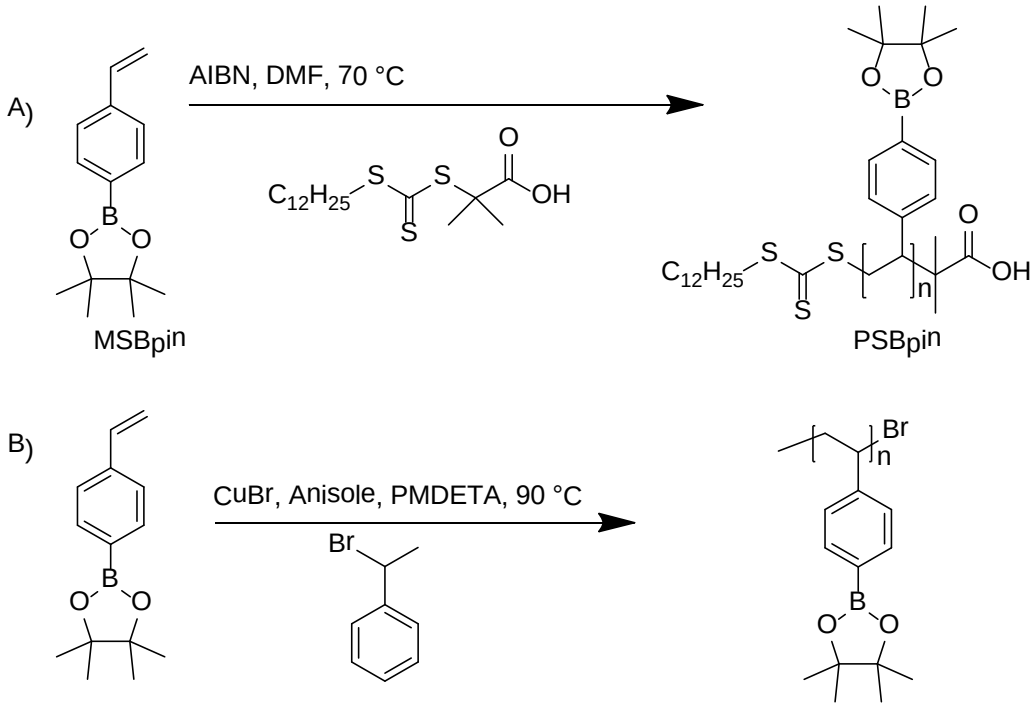

Figure 1.3
Boron pendent chain polymers via ATRP or RAFT synthesis.

End functionalized organoboron polymers were synthesized using styrene, but by substituting either a boron functionalized CTA[19] for RAFT, or using a boronic acid precursor moiety to function as the ATRP initiator, **Figure 1.4**. Upon formation of PS-$SiMe_3$ borylation and aqueous workup gave end functionalized PS-$B(OH)_2$[20].

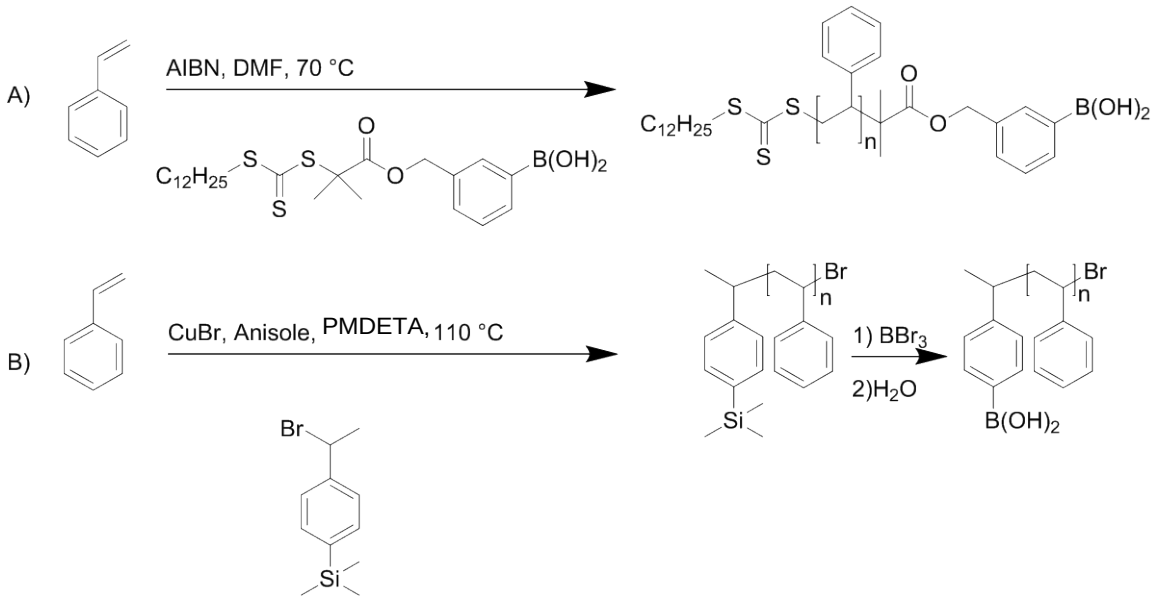

Figure 1.4
Organoboron end functionalized polymers using A) RAFT Polymerization Technique and B) ATRP[9] Polymerization Technique.

As previously mentioned, the overall goal of this work was to develop and characterize novel COFs, which maintained the -18Å diameter, while improving hydrolytic stability. The first route to modifying the surface of the COF is in **Chapter 3**. Large macromolecular Lewis base containing polymers were grafted to the surface COF sheets, where the Lewis basic polymer binds to the Lewis acidic COF. Now that these orbitals on the boronate COF sheet are occupied, displacement and hydrolysis is retarded.

Lastly, **Chapter 4** will highlight some post polymerization modifications taking advantage of the terminal diols that are exposed on the exterior of the COF particles. These "end groups" can covalently bond to a boronic acid and form another aryl boronate ester linkages. Both end functionalized boronic acids and pendent chain boronic acid polymers were prepared, and were attempted to graft to the COF. The most promising

way to modify the COF was for an insitu formation of a COF-18Å, followed by esterification of the terminal diols using a boronic acid pendant polymer. The incorporation of polymer improved the stability, while maintaining porosity.

1.3 References

1. Yaghi O., M.; O'Keeffe M.; Ockwig N., W.; Chae H., K.; Eddaoudi M.; Kim J. Reticular Synthesis and The Design of New Materials. *Nature* **2003**, *423*, 705-714.

2. Cote, A. P.; Benin, A. I.; Ockwig, N. W.; O'Keeffe M.; Matzger, A. J.; Yaghi O., M.; Porous, Crystalline, Covalent Organic Frameworks. *Science* **2005**, *310*, 1166-1170

3. Sudik, A.; Ockwig, N.; Cote, A.; Kim, J.; Yaghi, O. Design, Synthesis, Strcture, and Gas (N2, Ar, CO2, CH4 and H2) Sorption Properties of Porous Metalorganic Tetrahedral and Hetrocuboidal Polyhedra. *J. Am. Chem. Soc.* **2005**, *127, 7110-7118.*

4. Milwar, A.; Yaghi, O. Metal-Organic Frameworks with Exceptionally High Capacity for Storage of Cabon Dioxide at Room Temperature. *J. Am. Chem. Soc.* **2005**, 127, 17998-17999.

5. Saha, D.; Deng, S. Structural Stability of Metal Organic Framework MOF-177. *J. Phys. Chem. Lett.* **2010**, *1*, 73-78.

6. Kandambeth, S.; Mallick, A.; Lukose, B.; Mane, V., M.; Heine, T.; Banerjee, R. Construction of Crystalline 2D Covalent Organic Frameworks with Remarkable Chemical (Acid/Base) Stability via a Combined Reversible and Irreversible Route. *J. Am. Chem. Soc.*, **2012**, *134*, 19524–19527.

7. Kandambeth, S.; Shinde, B., D.; Manas, K.; Panda, L., B.; Lukose, B.; Heine, T.; Banerjee, R Enhancement of Chemical Stability and Crystallinity in Porphyrin-Containing Covalent Organic Frameworks by Intramolecular Hydrogen Bonds. *Angew. Chem. Int. Ed.* **2013**, 52, 13052–13056.

8. Tilford, R. W.; Gemmill, W. R.; zur-Loye, H.-C.; Lavigne, J. J. Facile Synthesis of a Highly Crystalline, Covalently Linked Porous Boronate Network. *Chem. Mater* **2006**, *18*, 5296-5301.

9. Tilford, R. W.; Mugavero, J. S.; Pellechia, J. P.; Lavigne, J. J. Tailoring Microporosity in Covalent Organic Frameworks. *Adv. Mater.* **2008**, *20*, 2741-2746.

10. Lanni, M. L.; Tilford, R. W.; Bharathy, M.; Lavigne, J. J. Enhanced Hydrolytic Stability of Self-Assembling Alkylated Two-Dimensional Covalent Organic Frameworks. *J. Am. Chem. Soc.* **2011**, 133, 13975-13983.

11. Christinat, N.; Croiser, E.; Scopelliti, R.; Cascella, M.; Rothlisberger, U.; Severin, K. Formation of Boronate Ester Polymers with Efficient Intrastrand Charge Transfer Transitions by Three-Component Reactions. *Eur. J. Inorg. Chem.* **2007**, 5177-5181.

12. Du, Y.; Mao, K.; Kamakoti, P.; Ravikovitch, P.; Paur, C.; Cundy,S.; Li, Q.; Calabro, D. Experimental and computational studies of pyridine-assisted post-synthesis modified air stable covalent–organic frameworks. *Chem. Commun.* **2012**, *48*, 4606-4608.

13. Du, Y.; Mao, K.; Kamakoti, P.; Wooler, B.; Cundy, S.; Li, Q.; Ravikovitch, P.; Calabro, D. The effects of pyridine on the structure of B-COFs and the underlying mechanism *J. Mater. Chem. A*, **2013**, *1*, 13171-13178.

14. Moad,G.; Rizzardo, E.; Thang, S.H. Living Free-Radical Polymerization by Reversible Addition-Fragmentation Chain Transfer: The RAFT Process. *Macromolecules.* **1998**, *31*, 5559-5562.

15. Wang, J. S.; Matyjaszewski, K. Controlled/"living" radical polymerization. Atom Transfer Radical Polymerization in the Presence of Transition-metal Complexes. *J. Am. Chem. Soc.* **1995**, *117*, 5614-5615.
16. Qin, Y.l;, Sukul, V.; Pagakos, D.; Jakle F.; Preparation of Organoboron Block Copolymers via ATRP of Silicon and Boron-Functionalized Monomers. *Macromolecules.* **2005** *38*, 8987-8990

17. Cambre, J.; Roy, D.; Gondi, R.; Sumerlin B. Facile Strategy to Well-Defined Water-Soluble Boronic Acid (Co)polymers. *J. Am. Chem. Soc.* **2007**, *129*, 10348-10349.

18. Qin, Y.; Cheng, G.; Achara, O.; Parab, K.; Jakle, F. A New Route to Organoboron Polymers via Highly Selective Polymer Modification Reactions. *Macromolecules*. ***2004***, 37, 7123-7131.

19. Sudershan, D., P.; Gondi, S.; Roy, D.; Sumerlin, B. Boronic Acid Terminated Polymers: Synthesis by RAFT and Subsequent Dynamic Covalent Self-Assembly. *Macromolecules.* **2009**, *42*, 5614-5621.

20. Qin, Y.; Cui, C.; Jakle F. Silylated Initiators for the Efficient Preparation of Borane-End-Functionalized Polymers via ATRP. *Macromolecules* **2007,** *40*, 1413-1420.

21. Farha, K.O.; Yazaydin O.; Eryazici, I.; Malliakas, D. C.; Hauser, G. B.; Kanatzidis, G. M.; Nguyen, T. S.; Snurr, Q. R.; Hupp, T. J. De novo Synthesis of

a Metal-Organic Framework Material Featuring Ultrahigh Surface Area an Gas Storage Capacities *Nature Chemistry* **2010**, *2 944-948.*

CHAPTER 2: Synthesis of Covalent Organic Frameworks

2.1 Overview

COFs are synthesized from a trifunctional boronic acid moiety and a tetrol in a condensation polymerization as shown in **Figure 2.1**. Due to the reversibility of the boronate ester linkages hexagonal sheets are possible[1]. Previous group members calculated the typical length of a COF sheet repeat unit, as a tenmer. These sheets are then able to pi-pi stack in approximately 10 high. In addition, previous group members were able to tailor the porosity of these frameworks by introducing alkyl chains on the tetrol[2].

One interesting change in the structure-property relationship was that these hydrophobic chains, increased COFs hydrophobicity, which decreased the propensity of the weak hydrophilic nucleophiles from attacking the top sheet empty p-orbital on the boronate esters[3]. The focus on this chapter was to develop a method to facilitate the COF synthesis. In order to obtain the thermodynamic product, long reaction times are required, 72 hours, plus an additional 3 days to purify the material. An alternative method was developed by the Cooper group[4]. They showed that it is possible to decrease the reaction time by carrying the synthesis out in a microwave reactor. The following research investigated the synthesis of COF-18Å, which was subsequently characterized using ^{13} Carbon Cross Polarization Nuclear Magnetic Resonance (^{13}C CP-

NMR), Powder X-ray diffraction (PXRD), Gas Adsorption, and BET treatment (surface area)

2.2 Conventional Synthesis

Figure 2.1 shows the required reticular synthesis building blocks to form a COF. Methanol is used as a catalyst, which helps to dissolve the boronic acid and form a boronate ester. Once this boronate ester is dissolved, a facile condensation polymerization occurs. Methanol and the byproduct water are instrumental in forming the product due to the reversibility of the boronate ester. These byproducts form as the boronic acid is converted to the boronate ester. If the framework contains imperfections in connectivity from either cross-linking or cyclization of the boronate ester not occurring then these small molecules, either water or methanol, can help to hydrolyze these bonds. This hydrolysis occurs due to the reversibility of the boronate ester bonds, where water and methanol can help to yield the thermodynamically favored product. Previous group members showed that reaction times of 72 hours are required, this follows the Carother's Equation and the reaction required 1 mmol BTBA in 12 mL of solvent in order to obtain the highly crystalline and porous framework in high yields.

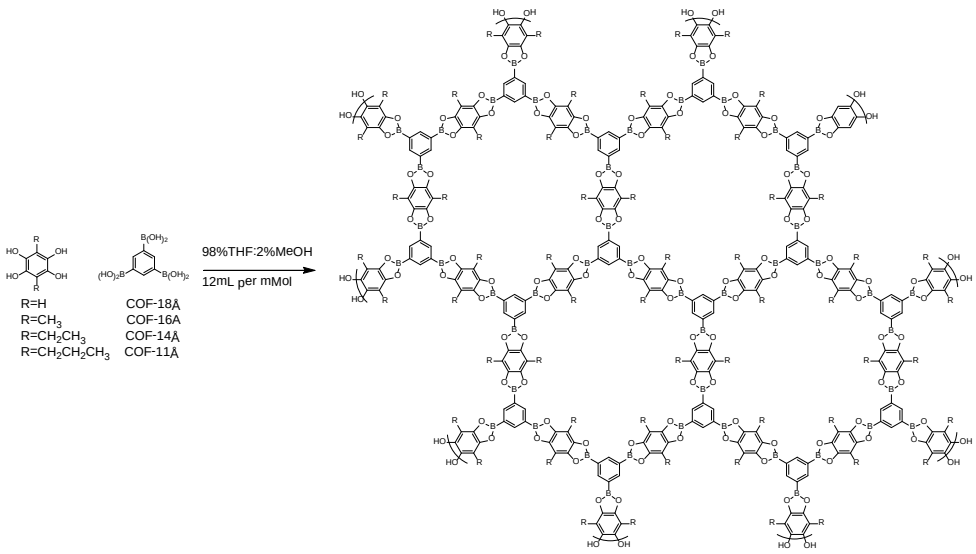

Figure 2.1
Scheme of the conventional synthesis of COFs: COF-18Å, COF-16Å, COF-14Å, COF-111Å,

2.3 Microwave Synthesis

To shorten synthetic time efforts made toward synthetizing COF-18Å in a microwave reactor. It has been reported that COF-5 was synthesized in 20 minutes using a CEM S- Class Explorer 96-posititon microwave reactor at 100°C and a power of 200 W. Using a CEM Discover-SP W/ACTIVENT, we investigated the formation of COF-18Å in 20 minutes, however, PXRD did not indicate synthesis of the porous framework. Optimization of this reaction to obtain the network included sparging the vessel with nitrogen for 30 minutes, diluting the monomer to solvent ratio to 1 mmol of BTBA per 20 mL (98%THF: 2%MeOH) and performing the polymerization for one hour, **Figure 2.2**. Further optimization is required including longer time and lowering the concentration of solvent, as the yield of COF-18Å was only 48%. Copious rinsing afforded the activated

COF-18Å with no apparent monomer trapped in the pores which was confirmed using PXRD and ^{13}C CP-MAS NMR.

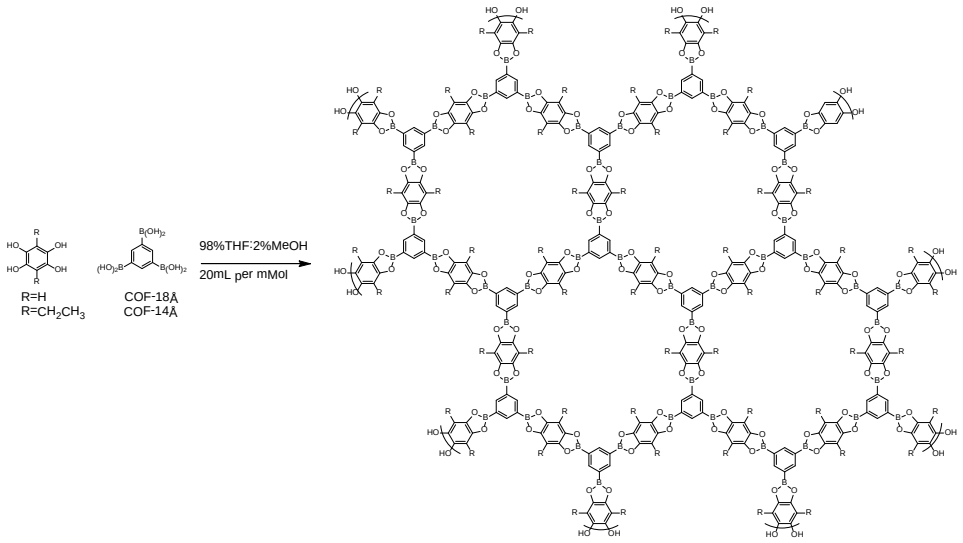

Figure 2.2
Reaction Scheme to synthesize COF via a microwave reactor

2.4 COF-18Å Characterization

The first technique required to characterize the frameworks was PXRD shown below in **Figure 2.3A.** Both materials contain the desired peaks (h, k, l) at the (1,0,0), (1,1,0), 2,0,0) and (0,0,1). The preferred orientation of COF-18 Å is that the intensity (1, 0, 0) is larger than the (0, 0, 1) 3.5Å, a cartoon depicting these axis are shown in **Figure 2.3B**. The 100 powder peak materials were characterized on different instruments, making a direct comparison difficult. The center to center distance going across the lattice is indicative of the 18Å framework formed, whereas, the 001 peak is distance between the sheets. Solving for Bragg's Law, the 001 distance is around 3.5Å, which is consistent with the height of two benzene molecules pi stacking on top of each other. The

rest of the PXRDs mentioned in this thesis, were normalized from the 100 peak. If small molecules are encapsulated in the pores, then a diffraction pattern will arise between 15 and 20 degrees two Θ.

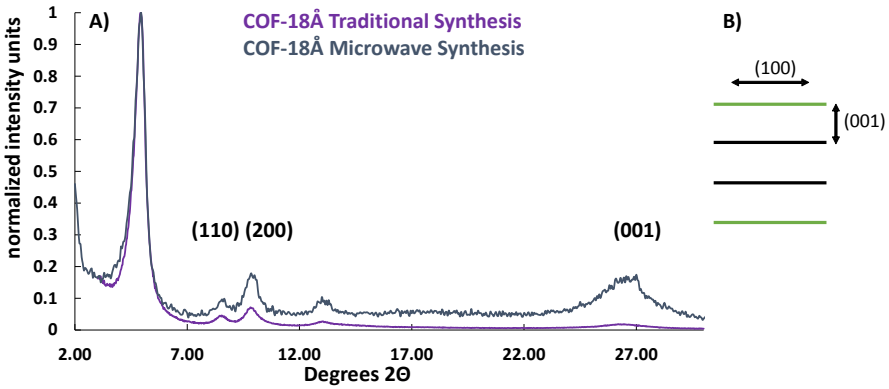

Figure 2.3

A) Overlaid PXRD patterns of COFs obtained by either a traditional synthesis, purple or from a microwave synthesis, blue-gray. **B)** Cartoon to depict the 100 peak, green, and the 001 peak, black.

The next tool used for characterizing these frameworks was MAS ^{13}C CP-MAS NMR. The NMR spectra are shown in **Figure 2.4**. **Figure 2.4A)** is the COF-18Å that will be referred to as the Copious COF-18Å batch from the traditional synthesis, and all subsequent modifications were carried out using this material. This spectrum contains 4 different carbon resonances which is interesting because the ipso boronic acid carbon is not expected to be observed due to the quadrupolar boron, due to splitting[5] As a result, the two internal peaks are thought to be a repeat unit and an end group of COF-18Å from the long range ordering. The ratio between the repeat units, or internal sheets, and the end groups, or external sheets, may give some idea about long range order, and one can infer about surface area from this ordering. An NMR of

a lower quality COF-18Å was synthesized **Figure 2.4B**, where the repeat unit is starting to form, but the majority of the material is still an end group. The microwave **Figure 2.5C** COF-18Å was reacted for an hour, and it is possible that the polymerization did not go to high conversion. The lower conversion COF materials contained more end groups than repeat units, or less long range ordering.

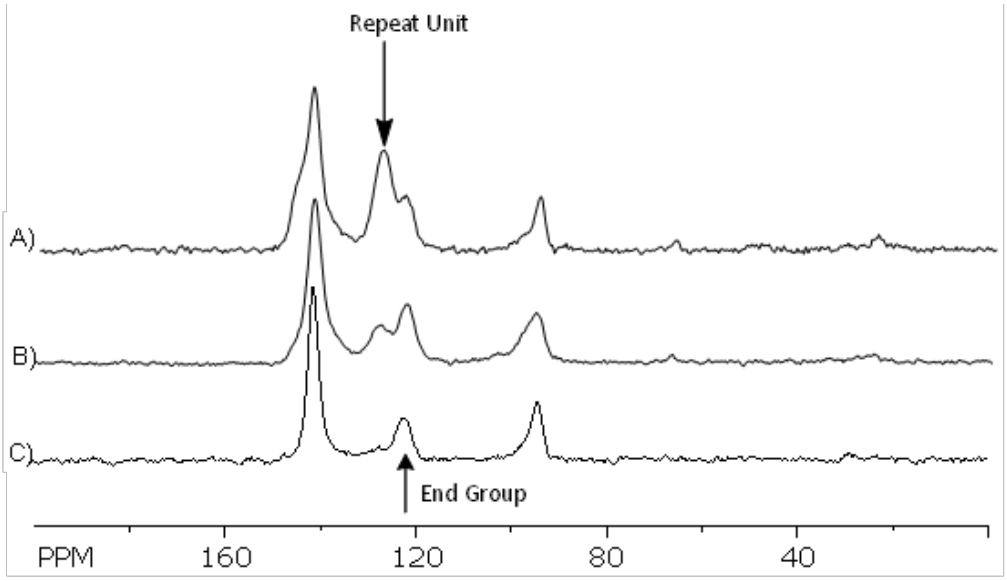

Figure 2.4
^{13}C CP-MAS NMR of **A)** and **B)** Traditional COF-18Å synthesis **C)** COF-18Å from microwave.

In order to test this hypothesis, nitrogen gas adsorption was run on both materials, and the results are shown in **Figure 2.5**. The blue lines represent the adsorption isotherm, and the desorption isotherm is colored in orange. **Figure 2.5A**) shows the adsorption and desorption isotherm of COF-18Å made the traditional way, whereas, **Figure 2.5B**) shows the isotherm for microwave COF-18Å. It is interesting to note that both materials contain a type one isotherm. Both the adsorption isotherm and desorption isotherm are the same, implying that no hysteresis is present or the mechanism of

desorption is the same mechanism as adsorption. And desorption mechanism are the same, this is observed due to the fact that both the adsorption. The microwave COF-18Å adsorbs less nitrogen, which goes along with the idea of being able to differentiate internal and external COF species in the ^{13}C-CP MAS NMR. The COF-18Å synthesized via the traditional route, the ^{13}C CP-MAS NMR shown in **Figure 2.4A** has the greatest long range ordering, and also has the ability to adsorb more nitrogen, isotherm is shown in **Figure 2.5A**, due to more COF stacks. However, the COF-18Å synthesized via a microwave reactor, ^{13}C CP-MAS NMR shown in **Figure 2.5A** has less long range order, or less stacks of COF, and it is expected to adsorb less nitrogen, which is the case and is shown in **Figure 2.5B**, where this material adsorbs less nitrogen, a larger picture of **Figure 2.5** is in **Appendix D**.

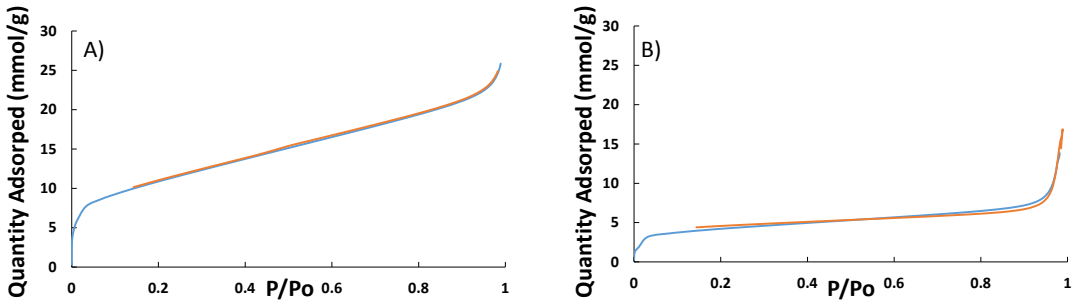

Figure 2.5

A) Nitrogen Adsorption, blue, and Desorption Isotherms, orange, of COF-18Å obtained from traditional synthesis and **B** of COF-18Å obtained from microwave.

To further evaluate surface area, the isotherms were subjected to BET treatment for the mesoporous range a P/P_o from .05-.3. COF-18Å has an 18Å diameter, the microporous range is <2Å, and the mesoprorous range is between 2Å and 50Å. Previous group members reported COFs surface area based on mesoporous range. Solving for the

mesoporous range from the BET treatment, **Figure 2.7**, shows that the microwave COF-18Å has a surface area about 400m^2/g where Copious COF-18Å material made the traditional way has a surface area of 900 m^2/g. The poorer quality COF-18Å synthesized from the traditional route a surface area between those two at around 700m^2/g.

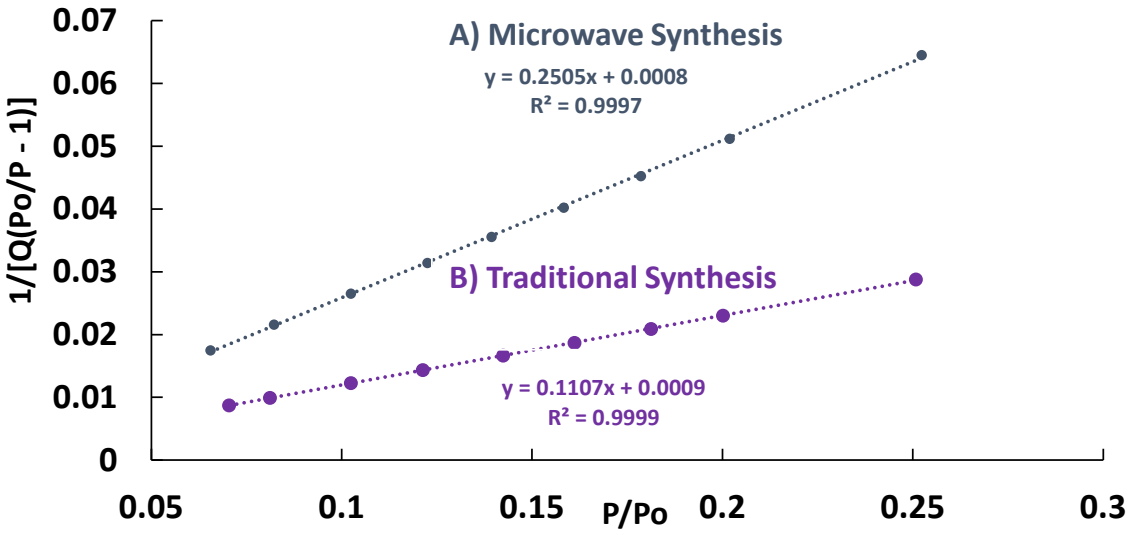

Figure 2.6
BET treatment from the Nitrogen isotherms of **A)** microwave synthesized COF-18Å, and **B)** traditionally synthesized COF-18Å.

2.5 Conclusion

In conclusion, we are able to synthesis COF-18Å using the traditional method and by a novel method, using a microwave reactor. Both methods yield porous materials with a type 1 isotherm. Future work would include optimization of the microwave method to produce higher surface area materials by reacting the material for longer times. It was advantageous to discover a way to relatively determine surface area by ^{13}C CP-MAS NMR. The relationship between surface area and internal/external layers resulted

in a nonlinear relationship, but NMR spectroscopy allows for a facile way to determine surface area due to the relative intensities of the COFs internal and external sheets.

2.6 Experimental

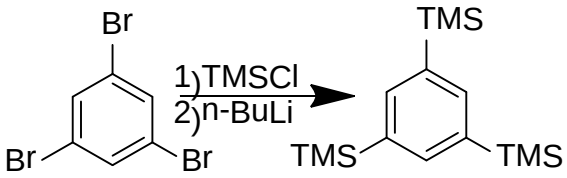

Figure 2.7
1,3,5, tris(trimethylsilyl)benzene scheme

Synthesis of 1,3,5-tris(trimethylsilyl)benzene. To a stirring solution of 1,3,5-tribromobenzene (5.0 g, 15.8 mmol) in THF (30 mL), trimethylsilylchloride (25.7 g, 237 mmol) was added. The mixture was cooled to -78 ºC (acetone/dry-ice bath) and *n*-BuLi (53 mL, 1.4 M in hexane, 97.8 mmol) was added drop-wise over 1 h. The resulting solution was kept at -78 ºC, and was allowed to warm to 25 ºC overnight. The reaction mixture was cooled to 0 ºC (icebath) and quenched with water. To the solution ethanol was added to facilitate azeotropic removal of water/THF. The crude material was purified by extraction with aqueous NH_4Cl solution (50 mL) and extracted with CH_2Cl_2 (3 × 50 mL). The organic layers were combined, dried over $MgSO_4$, and then concentrated to a minimum. The workup afforded 1,3,5-tri(trimethylsilyl)benzene (4.23 g, 90%) as a red oil. ^{1}H NMR (300 MHz, $CDCl_3$): δ 7.7 (s, 3 H) 0.40 (s, 27 H,). [13]

[13] If crystals are present after distillation and material crystallizes, the material is impure.

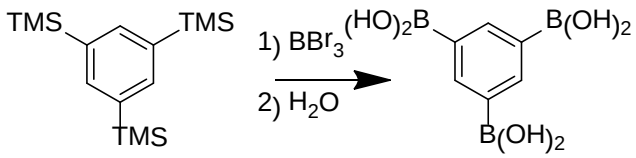

Figure 2.8
1,3,5 Triboronic acid synthesis

Synthesis of 1,3,5-tris Triboronic Acid. 1,3,5-Tris(trimethylsilyl)benzene (1.75 g, 5.95 mmol) was treated with excess neat boron tribromide (7.8 g, 31.14 mmol) under dry nitrogen. The solution was heated to reflux for 4 h. Once cooled, solution was cooled to -78 ºC (dry ice/acetone) excess boron tribromide was removed via sublimation, solution was kept at -78 ºC. Hexane (50 mL) was added, and solution was cooled to 0 ºC (ice bath). Water was slowly added dropwise, while stirring until reaction was quenched. Solid was collected by filtration and rinsed with water. Compound was covered and air dried for 72 h. The workup afforded 1,3,5-triboronic acid (0.886 g, 90%) as a gray powder. ^{1}H NMR (300 MHz, 1M KOH in Dw_2O): δ 7.30 (s, 3 H,).

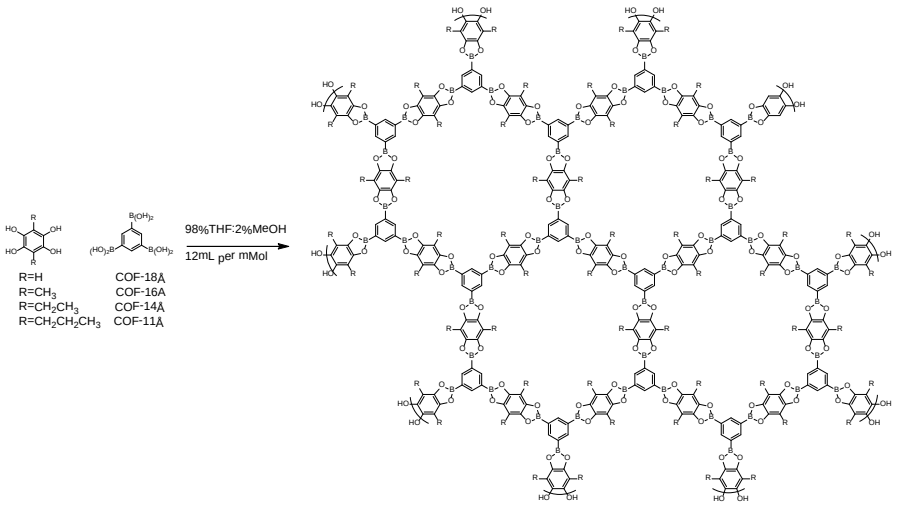

Figure 2.9
Traditional Synthesis of COF

Synthesis of COF-18Å via Traditional Synthetic Route. Benzene-1,3,5-triboronic acid (0.907 g, 3.44 mmol) and 1,2,4,5-tetrahydroxybenzene (1.07 g, 7.55 mmol) were dissolved in THF (41.2 mL) and methanol 0.8 mL). The solution was heated to reflux under nitrogen for 72 h. The mixture was cooled to room temperature and the precipitate was collected and rinsed with THF (50 mL). The solid was placed under vacuum for 72 h. The workup afforded COF-18Å (1.04 g, 84 %) as a powder.

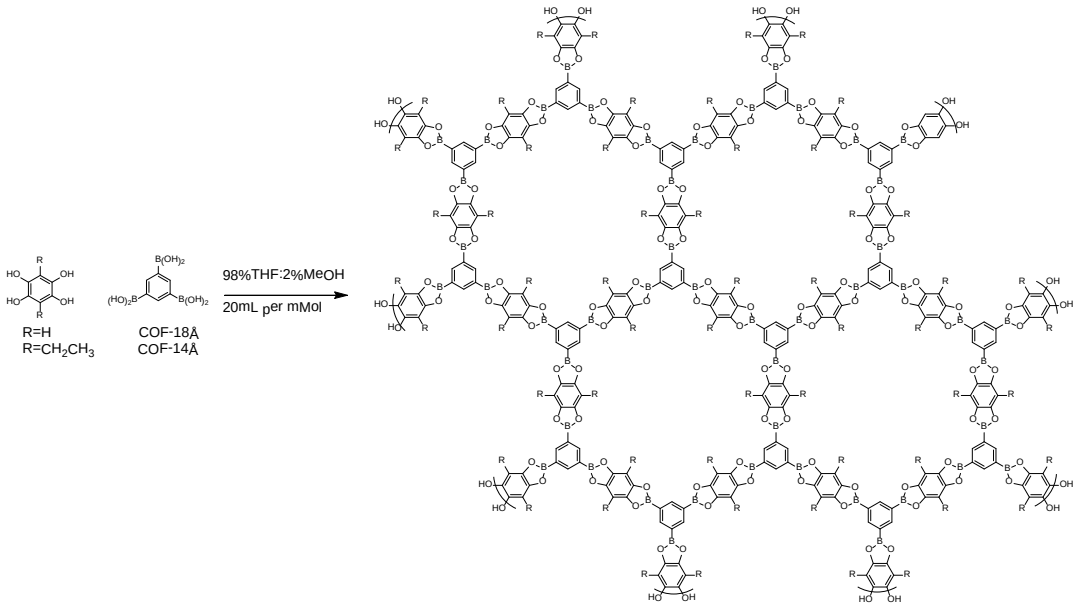

Figure 2.10
Microwave Synthesis of COF.

Synthesis of COF-18Å via Microwave Synthetic Route. Benzene-1,3,5-triboronic acid (0.260 g, 1 mmol) and 1,2,4,5-tetrahydroxybenzene (0.312 g, 2.19 mmol) were dissolved in THF (19.8 mL) and methanol 0.2 mL). The solution was sparged under constant flow of nitrogen for 0.5 h. The reaction mixture was heated to 105 ºC for 1 h. The vessel was allowed to cool to room temperature and the precipitate was collected and rinsed with

THF (150 mL). The solid was placed under vacuum for 24 h affording a powder. The workup afforded COF-18Å (0.109 g, 48 %) as a powder.

General Procedure for Activation of COFs. COFs were activated for analysis by suspending COF in dry THF (50 mL). After 24 h, the supernatant was removed and additional THF was added to the round bottom. After another 24 h, the supernatant was decanted and the sample was dried on a vacuum line at ambient temperature for 16 h. The resulting dried powder was ground with mortar and pestle for immediate use.

Gas Adsorption Analysis: Gas adsorption data was collected using a liquid nitrogen bath for nitrogen adsorption isotherm. The dried powder was loaded into a 6 mm sample cell (small bulb) and degassed at 250 ºC under high vacuum (<0.001 mm-Hg) for 2.5 h.

2.7 References

1. Tilford, R. W.; Gemmill, W. R.; zur-Loye, H.-C.; Lavigne, J. J. Facile Synthesis of a Highly Crystalline, Covalently Linked Porous Boronate Network. *Chem. Mater* **2006**, 18, 5296-5301.
2. Tilford, R. W.; Mugavero, J. S.; Pellechia, J. P.; Lavigne, J. J. Tailoring Microporosity in Covalent Organic Frameworks. *Adv. Mater.* **2008**, 20, 2741-2746.
3. Lanni, M. L.; Tilford, R. W.; Bharathy, M.; Lavigne, J. J. M Enhanced Hydrolytic Stability of Self-Assembling Alkylated Two-Dimensional Covalent Organic Frameworks. *J. AM. Chem. Soc.* **2011**, 133, 13975-13983.
4. Campbell, N. L.; Clowes, R.; Ritchie, L. K.; Cooper, A. I. Rapid Microwave Synthesis and Purification of Porous Covalent Organic Frameworks. *Chem. Mater* **2009**, 21, 204-206.
5. Rambo, M. B.; Lavigne, J. J. Defining Self-Assembling Linear Oligo(dioxaborole)s. *Chem. Mater.* **2007,** *19*, 3732-3739

CHAPTER 3: Synthesis of Face Modified Covalent Organic Frameworks

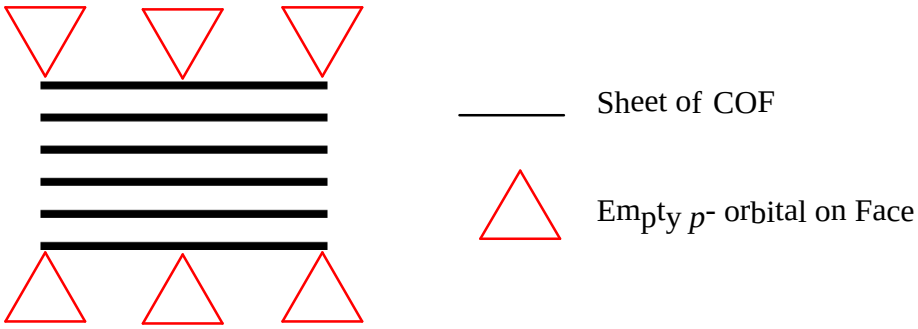

Figure 3.1
Cartoon to visualize where face modification occurs.

3.1 Overview

The hydrolytic stability of COF-18Å can be tailored, by reacting a Lewis base with an a Lewis acidic COF. It has been reported in the literature that decorating the COFs surface with a Lewis base monomer will improve the stability, by using side chain polymers containing the Lewis base functionality.[1 2] These newly functionalized COFs were compared to nonalkylated COF-18Å. When these materials interact, three possibilities are available. These modifications are outlined in **Figure 3.1**. The first outcome **Figure 3.1A** is if the polymer goes into the porous framework without a chemical reaction occurring, forming a physical mixture. The second outcome, **Figure 3.1B** is a chemical reaction between both the internal surface sheets of the COF-18Å, and the internal surface sheets of the COF-18 Å. This could occur because both layers are

comprised of sp^2 hybridized boronte esters, which could be problematic due to the COF-18Å sheets delaminating, or if the polymer is intercalated between the COF-18Å sheets. The third outcome, **Figure 3.1C**, would occur if the polymer reacted with the external layers only, and resulted in a surface modification.

Results indicated surface modification as shown in **Figure 3.1C** was the most likely outcome. This was further confirmed through ^{11}B NMR and PXRD. ^{11}B NMR showed 15% coordination with an equal molar ratio of 1COF-18 Å:1P(4VP). When the polymer was added in a fourfold excess, the amount of coordination stayed at 15%. If delamination or intercalation occurred then the amount of coordination should have increased drastically. To further validate, PXRD showed that the (001) diffraction pattern remained; proving pi-pi stacking remained after post-polymerization modification.

Synthesis and characterization of these newly formed materials will be discussed first in this chapter, followed by investigation of their respected properties. The properties will be analyzed with respect to nitrogen adsorption, and hydrolytic stability. The first variable investigated was the method of preparation (vortex, lower boiling solvent, and higher boiling point solvent). The other variables investigated were impact of molecular weight of the pyridine material, as materials get larger their properties change (i.e. methane, octane, and undecane, are a gas, liquid and a solid respectively). Finally, varying grafting density (boron-nitrogen ratio) ratios were investigated

Table 3.1 Overview of COF-18Å derivatives synthesized and comparisons to be formed.

COF	Preparation	Molecular weight	Grafting density
COF+Pyridine		B	
1COF:1P4VP Vortexed	A		
1COF:1P4VP from DCM	A		
1COF:1P4VP from dioxane	A	B	C
1COF:1P4VP*from dioxane		B	
1COF:5P4VP			C
1COF:2P4VP			C
2COF:1P4VP			C
5COF:1P4VP			C

*higher molecular weight polymer, 160k all others are 60k. A) represents the preparation method B) molecular weight C) grafting density.

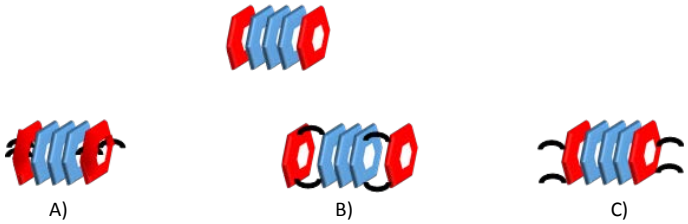

Figure 3.**2**

This schematic depicts all likely eventualities, when COF-18 Å and a pyridine containing compound interact, Red hexagons represent the external layers, and blue hexagons represent the internal layers. Figure A) represents a physical mixture between the materials where no actual bonds are formed, as a result, the pyridine molecules may penetrate into the COF-18 Å pores, or a heterogeneous material of COF-18Å and pyridine are possible. Figure B) since all layers of COF-18 Å are formed due to pi-pi stacking interactions, the pyridine may intercalate into the other sheets. The last eventuality is C) where the Lewis base coordinates to the external COF-18Å layer.

3.2 Results and Discussion

The focus of the research was to gain insight on the structure-property relationship between Lewis acidic COF-18A and Lewis basic pyridine. COF-18Å is comprised of numerous sp^2 hybridized boronate species. This material is formed through a condensation reaction between a diol and boronic acid. After the reaction, boron will still contain an empty p orbital, which upon coordination to pyridine form sp^3 hybridized sheets. The change in hybridization is formed by a dative bond, which forms from the lone pairs of electrons from pyridine and the empty p orbital on boron.

Workup showed when rinsing these materials with organic solvent the pyridine polymer would re-disperse into the solvent, disrupting the dative bond. This resulted in only recovering the COF-18Å. The materials discussed herein were synthesized without a workup step.

3.2.1 COF CHARACTERIZATION

The first characterization technique implemented was solid state ^{13}C MAS NMR **Figure 3.2** is a spectra of COF-18Å + anhydrous pyridine, that showing signals representing only the aromatic resonances of COF-18Å. This material was stored under ambient conditions overnight in an NMR rotor. Concurrently, the remainder of the COF-18Å + anhydrous pyridine material was placed in a vacuum oven overnight to remove the free pyridine molecules encapsulated in the pores. **Figure 3.2B**, after storing overnight in an NMR rotor, the material contains a small percentage of carbonyl resonances implying that the boronate esters were slowly hydrolyzing, and the THB monomer was autoxidizing into quinone, this Resonance has a chemical shift of 180PPM.

In **Figure 3.2C**, the material was then out gassed at reduced pressure and 250 ^{o}C for 2.5 h. The resulting material contained no carbonyl peaks, implying the material present was only COF-18Å /pyridine material. However, ^{13}C CP-MAS NMR did not elucidate whether the pyridine was bound to the COF-18Å due to the fact that the molar ratio of pyridine to COF-18Å is very low.

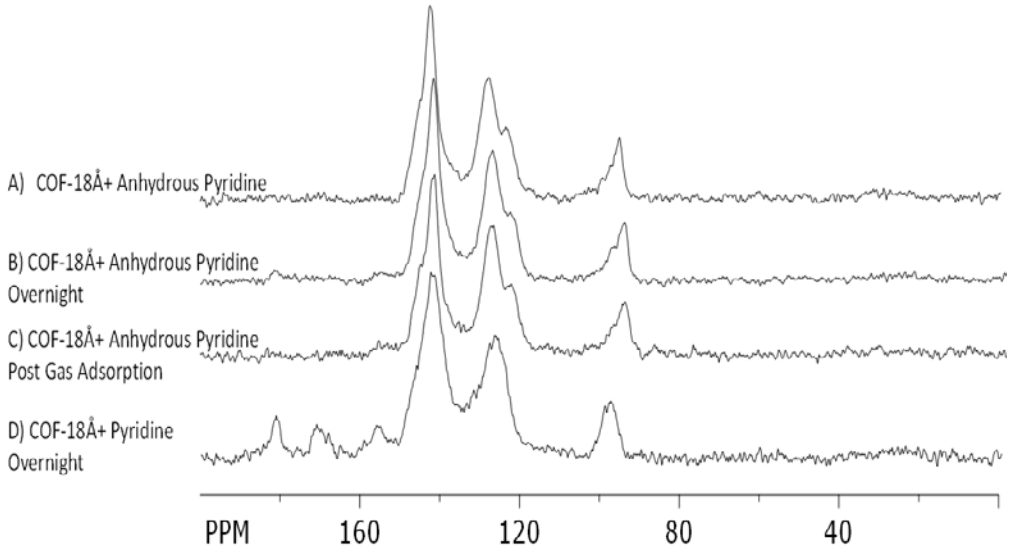

Figure 3.3

^{13}C CP-MAS NMR of small molecule pyridine functionalized COF-18 Å.

After learning that the dative bond would not facilitate hydrolysis, the size of the monomer was increased to poly(4-vinyl pyridine), P(4VP), 60k. The initial studies focused on characterizing the material based on various synthetic procedures using a 1COF:1P(4VP) molar ratio, **Figure 3.3**. **Figure 3.3 B** and **Figure 3.3C** indicate that the carbons in these materials are in a similar environment. **Figure 3.3D** shows a significant change in two resonances. The first is the intensity increase of the downfield peak, which was identified to be the unsubstituted carbon from THB. In addition, there was a change in peak intensity height of the two peaks between 120-130 ppm. The up field peak (~123

ppm) corresponds to the external layer of the COF repeat unit, and the more downfield internal peak ~130 ppm corresponds to the internal units. See chapter 2 for a complete discussion. This is consistent with the hypothesis of a surface modification on the exposed external layers.

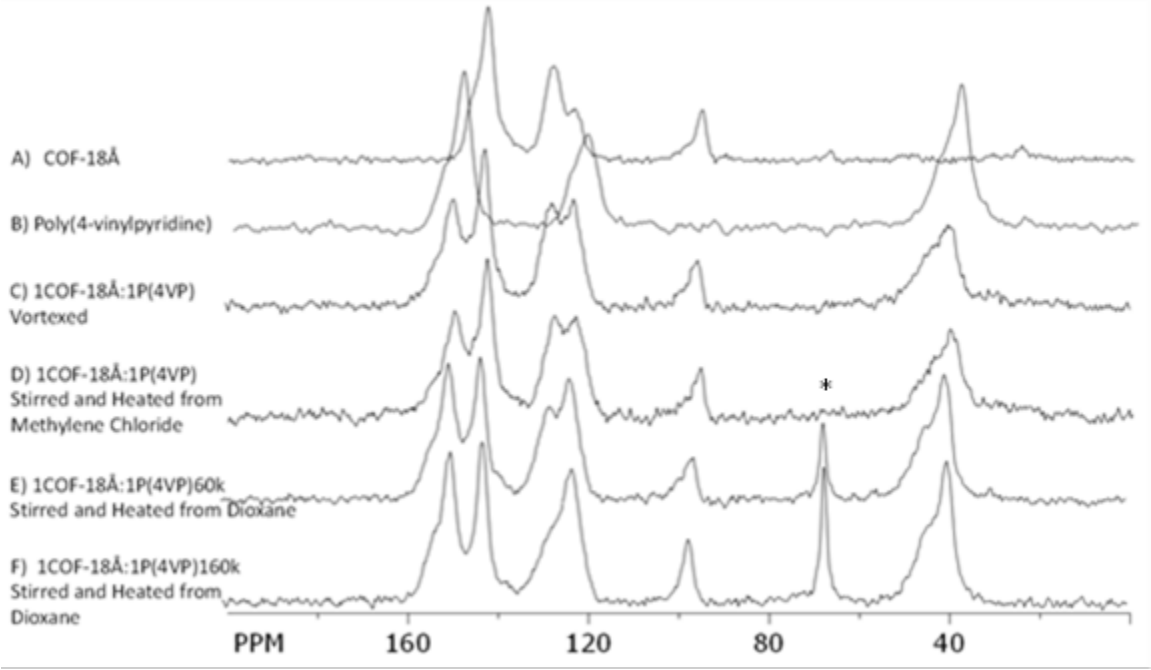

Figure 3.4

^{13}C CP-MAS NMR Spectrum of face modified material, various synthetic routes. * is residual dioxane at 70PPM, which is either trapped in the pores of the COF-18Å, or are entrapped in the long polymer chains.

Next, the impact of grafting density was studied. The salient feature is that the relative intensities of the COF-18Å and P(4VP) change as the ratio between these two are varied as shown in **Figure 3.4**. These NMR spectra did not indicate whether the material was a physical mixture or a modified COF.

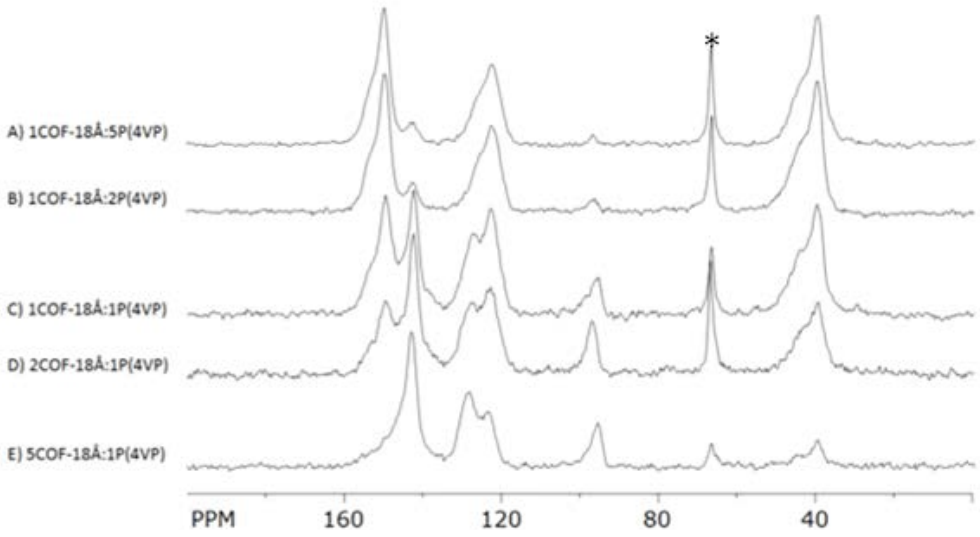

Figure 3.5

^{13}C CP-MAS NMR Spectrum of face modified material with different grafting densities. * is residual dioxane at 70PPM, which is either trapped in the pores of the COF-18A, or are entrapped in the long polymer chains.

3.2.2 ^{11}B MAS NMR

^{11}B MAS NMR was performed to attempt to answer the question of whether the observed changes in **Figure 3.4** were actually from a chemical reaction, where the electrons on the pyridine molecule coordinated with the empty p orbital on the boronate ester. The resulting new bond would cause a change in the chemical environment and produce an additional NMR resonance. It is well known in the literature that ^{11}B NMR resonances are sensitive to hybridization, and all the COF-18 Å resonances are from sp^2 hybridized material.[2,3] The two different resonances arise from internal and external sp^2 environments, as the COF-18 Å material contains two separate boron components, see **Appendix A**.

Figure 3.5 is a representative ^{11}B NMR spectrum of these materials. Due to the 1.9mm NMR probe containing boron nitride, the resulting background resonance

collected from a blank collection (adamantane standard) was subtracted from all the collected spectra. After the background subtraction, spectra were fit with quadrupolar line shapes allowing for small changes to the anisotropic chemical shift. The deconvoluted spectra indicated how many different boron species were present, and allowed us to determine the ratio of boron species. With each spectral fitting the least number of boron components were used. Numeric output for all results are in **Appendix B**.

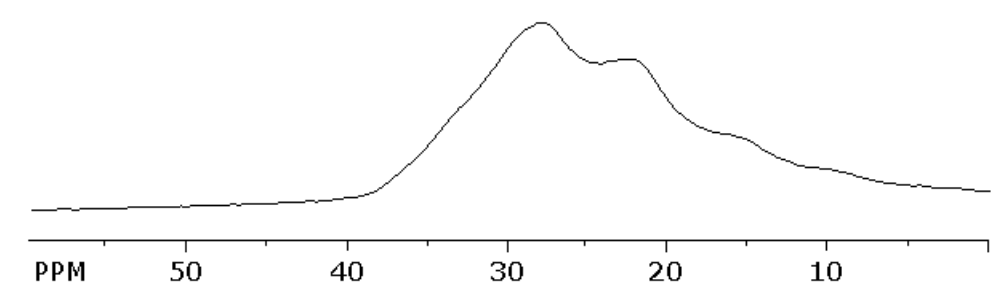

Figure 3.**6**
^{11}B NMR of COF18A + Anhydrous Pyridine before probe subtraction, and deconvolution.

The fitted spectra allow the determination of how many different boron species that are present (**Figure 3.6A)** in pristine COF-18Å, which was synthesized from BTBA and THB. The salient feature **in Figure 3.6B** is that as dative bond formation occurs the appearance of a new boron species is observed, species C. Resonance C is indicative of a sp^3 hybridized material, which formed when the lone pair of electrons on the pyridine molecule coordinates with the Lewis acidic boron external layer centers. This showed that the dative bond is formed quickly, when the pyridine lines up perpendicularly to the external layer of the COF-18Å, forming the tetrahedral sp^3 boron species.

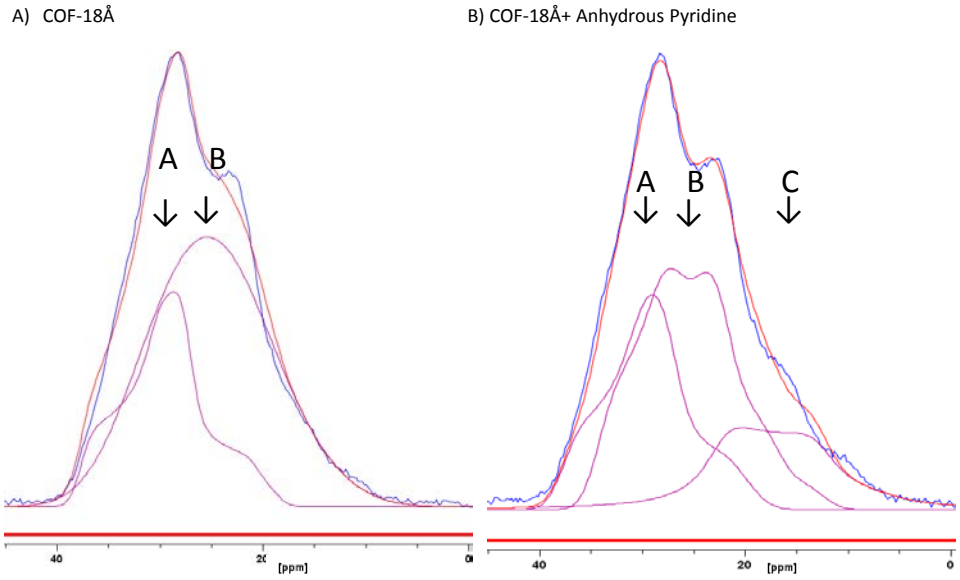

Figure 3.7

A) ^{11}B MAS NMR of COF-18Å after deconvolution. **B)** ^{11}B MAS NMR after deconvolution of COF-18Å and pyridine immediately after mixing the materials.

The COF-18Å /pyridine mixture initially contained 30% sp^3 character. After placing under reduced pressure overnight free and bound pyridine was removed, and the dative bond decreased by roughly 50%. The material stored in the rotor also had a decrease by 33%. The decrease most likely occurred from the reversible nature of the dative bond and evaporation of pyridine. After gas adsorption, the COF-18 Å /pyridine material was subjected to ^{11}B NMR, to answer if the weak bond could withstand the reduced pressure, and a high temperature environment. The results indicate that the material contained unreacted pyridine, which was not bound to the COF-18 Å, and it is possible under these harsh conditions, that the pi-pi stacking was destroyed, causing intercalation of the small molecule into the layers.

^{11}B NMR was very helpful in proving the hypothesis that the ^{13}C CP-MAS NMR studies were in fact correct, and that we were able to form two various physical mixtures, and a modified COF material. The first physical mixture was formed from vortexing the two materials and adding them together. Unlike the pyridine molecule which requires no heat, the larger polymers are unable to coordinate to the Lewis acidic centers. One possible reason is the solid polymers are random coils, and the probability of all the pyridine lone pairs of electrons being exposed and aligning perpendicularly to the COF-18Å are low. As a result, these two materials were dissolved and stirred in methylene chloride, to see if the dispersed polymer could easily coordinate to the exposed Lewis acidic centers. However ^{11}B MAS NMR and ^{13}C CP-MAS NMR showed that the material did not form sp^3 hybridized materials. As a result, a higher boiling point solvent was selected, i.e., dioxane. The higher boiling point solvent would allow for more energy to be introduced into the system. When these materials were stirred and heated in dioxane, the appearance of a new peak was observed as the hybridization changed from sp^2 to sp^3.

The percent incorporation remains around 15% for the various grafted density materials, which indicates that the large polymers are bound to the external layers of the COF-18Å, and the exposed external layers become saturated with low levels of pyridine. As a result, the excess pyridine polymer forms a physical mixture phase. This additional unreacted phase, contributes to the homogeneity of the samples. At this point, we know that all the face modified COF-18Å materials contain a sp^3 hybridized material with approximately 15% dative bond formation **Table 3.2**, however, which eventuality described in **Figure 3.1** remained unknown. To find out if these newly formed materials

had formed sp^3 hybridized materials on the surface or between the sheets, PXRD was implemented.

***Table* 3.2** Percent Coordination of Various Ratio COF

Name	% Coordination
COF-18 Å	0
COF-18 Å + Pyridine	30
COF-18 Å + Pyridine(overnight exposure)	20
COF-18 Å + Pyridine Pumped	17
COF-18 Å + Pyridine Post V	39
Any COF-18 Å:P(4VP) except*	15
1COF-18 Å:5P(4VP)*	25

***** indicates 1COF-18Å:5P(4VP) material.

3.2.3 PXRD

One way to determine where the modification occurred was to use PXRD. **Figure 3.7** shows a schematic of the COF-18Å framework, where the 100 peak goes across from the center of one repeat unit to the adjacent repeat unit. The 001 peak is the distance between the sheets, which forms when the COF-18Å sheets stack on top of each other due to pi-pi stacking. The PXRD shown below in **Figure 3.8A,** pristine COF-18Å, and the COF-18Å modified with pyridine, **Figure 3.8B**. The rest of the PXRD's are recorded in **Appendix C**. All PXRDs were normalized off of the 100 peak.

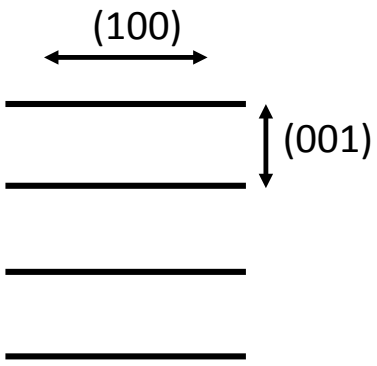

Figure 3.**8**
Representation of the different PXRD axis.

If intercalation, or defoliation occurred the center to center distance looking down the 001 axis should have shifted. Disruption in pi stacking, and incorporation of the pyridine molecule lone pairs of electron aligning perpendicularly to the boronate ester sheet would lead to the appearance of a peak at shorter 2theta. In order for the pyridine to coordinate with the internal or external layers, it must arrange where the lone pair of electrons on pyridine line up perpendicularly to the boronate ester. If the smallest molecule cannot intercalate into the COF-18Å then it would be very difficult for the larger polymers to do this. The main feature for these results is that the amorphous region increases as polymer ratio is increased, which is attributed to the amorphous polymer without sacrificing the integrity of the pi-pi stacking.

From the changes observed in the ^{13}C CP-MAS NMR, appearance of a third boron component in the ^{11}B NMR, and the fact the PXRD lacks a new 001 peak, the modification appears to have successfully worked on the surface. Next modification of the COF-18Å was carried out, and the bulk properties of these materials were investigated.

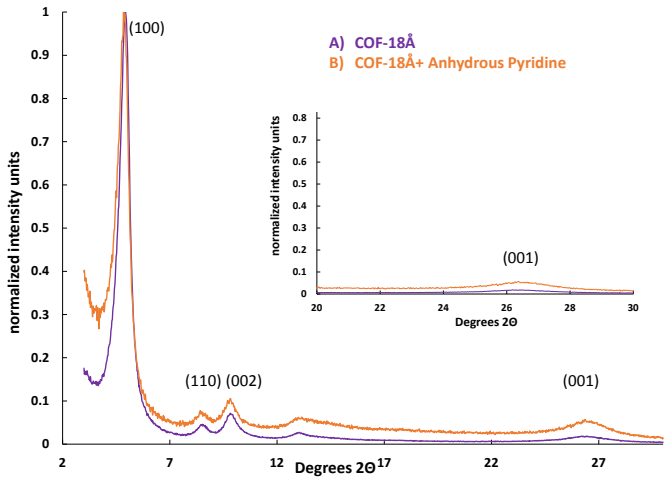

Figure 3.9
A) PXRD of COF-18Å before functionalization with a Lewis base. **B**) PXRD COF-18Å+ Anhydrous Pyridine.

3.3 Bulk Properties

Figure 3.9 contains nitrogen gas adsorption of COF-18Å modified with pyridine that resulted in a Type 1 isotherm, indicating that the material retains its microporous networks, with a much lower surface area using BET treatment. This finding was the antithesis of what is reported in the literature with respect to COF-5 decorated with pyridine molecules. The other modified isotherms materials are included in the A**ppendix D**. The various 1:1 ratio materials all contain a Type One isotherm, which is a knee shaped isotherm. The three 1:1 ratios saturated much faster than the physical mixture.

During the synthesis, the COF-18Å and P(4VP) were added at the same time, and then the heat was applied. It is possible that during this time the polymer may have went into the pores. After the reaction, these materials were outgassed on the autosorb-1 at 250 ^{o}C for 2.5 hours. At this temperature, the P(4VP) 60k was heated above its Tm, the

polymer was able to flow, and possibly disrupt the pi-pi stacking of the COF-18Å. After the run, the isotherm was analyzed with BET treatment from the relative P/P_o from .05-.3.

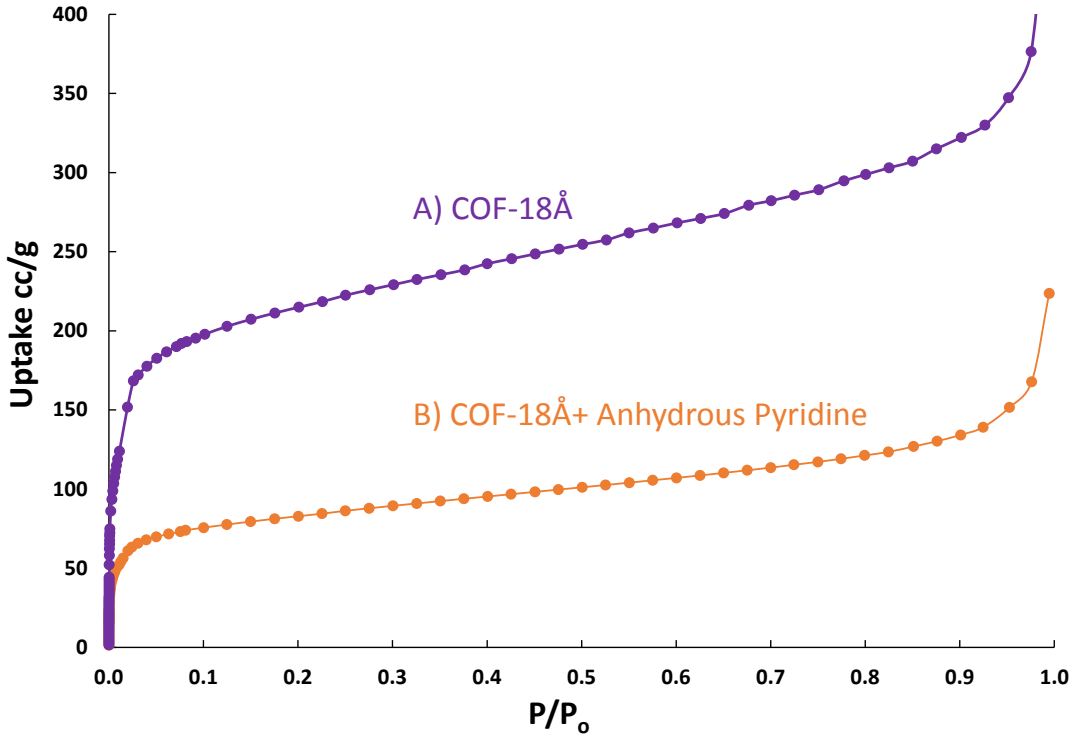

Figure 3.10
Nitrogen Adsorption of pristine A)COF-18Å and B) COF-18Å + Anhydrous Pyridine.

To calculate the surface area, the weight of P(4VP) was ignored due to the fact it had a negligible surface area of $16m^2/g$. The 5COF-18Å:1P(4VP) was optimized by running the same sample several outgassed at 250 ^oC for longer times. The times were 2.5 hours, 24 hours, and then an additional 26 hours, which had little impact in surface area. One question to be answered was whether these conditions could remove the dioxane trapped in the pores. **Figure 3.10A** shows the ^{13}C CP-MAS NMR of the 2COF-18Å:1P(4VP) material with all the dioxane removed. In addition, the two physical

mixtures composition appear to have changed. The physical mixture obtained by vortex **Figure 3.10B** looks like there is more polymer present and the stirred physical mixture **Figure 3.10C resembles** the 1COF-18Å:1P(4VP) from dioxane. To validate if this hypothesis is correct, these materials were again subjected to ^{11}B NMR. Both physical mixtures contain a third component, sp^3 hybridized boron species, see Appendix (B). This indicates that during outgassing the pyridine and COF react with one another.

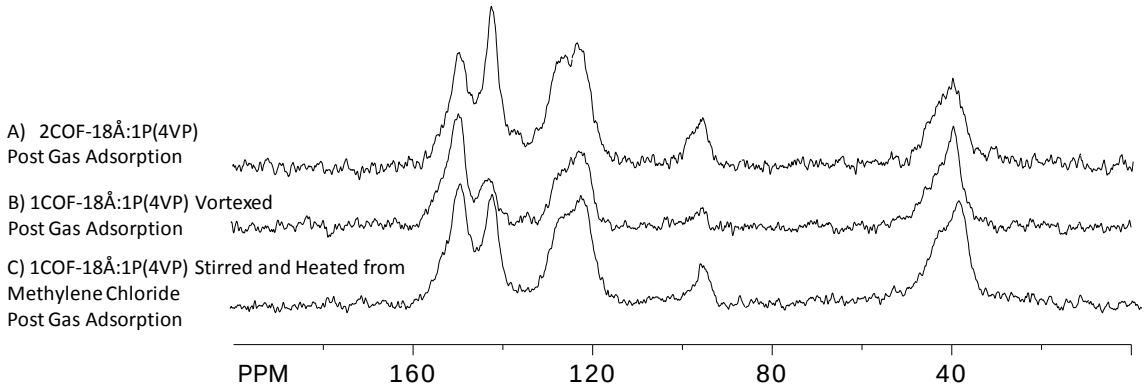

Figure 3.11

^{13}C CP-MAS NMR of COFs after gas adsorption. **A**) Shows that dioxane was removed. **B** and **C**) show that the materials are no longer physical mixtures with the 120 ppm peak intensity's changing.

Furthermore, as the size of the Lewis base increased: pyridine (4VP) 60k to P(4VP) 160k, the apparent surface area decreased. This trend is also seen with the decreasing the molar ratio of COF and increasing the ratio of polymer. As the amount of polymer increases, the apparent surface area decreases. It is important to restate the goals of the project, which were to maintain the 18Å diameter of COF, and not the surface area. The key difference is that porosity and surface area are two different measurements. Surface area takes into account both external surface and internal surface. One treatment of the isotherm, which can help answer this question is a thickness plot, t-plot, **Appendix**

F, if the material maintains the knee shape isotherm then it maintains porosity, a linear line through the origin shows no porosity. The material made by vortexing the polymer is a textbook example of a microporous material. The higher molecular weight P(4VP) material also maintains its porosity, due to the fact that the chains are longer, and thus the chances of these materials clogging the pores decreases. In addition, the 5COF-18Å:1P(4VP) and 2COF-18Å:1P(4VP) maintain porosity, and the other materials are hard to definitively group into this category.

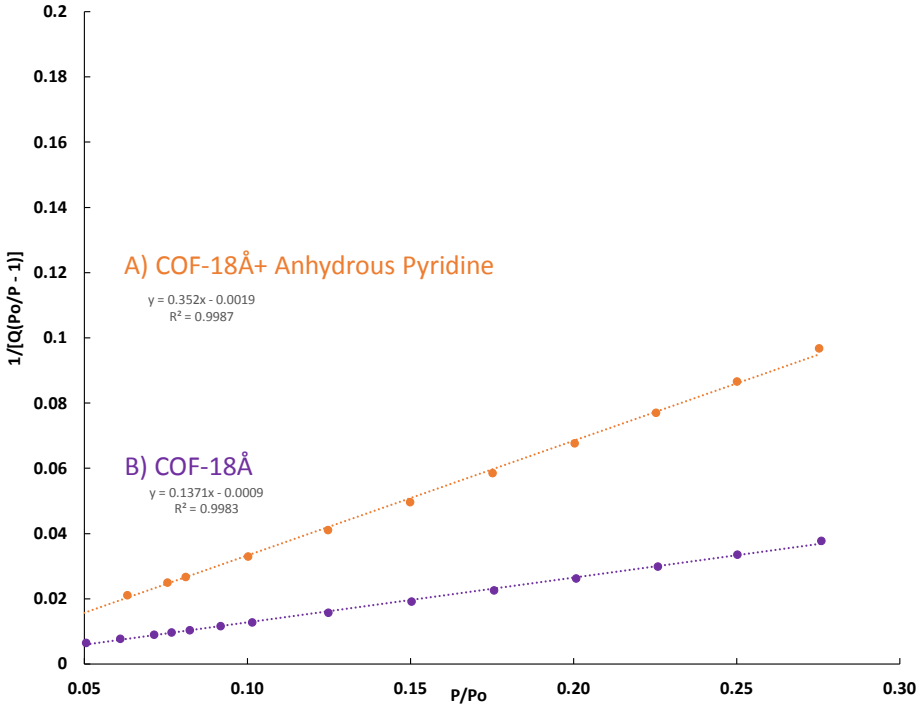

Figure 3.12
BET Treatment of pristine COF and functionalized COF, steeper the slope, less surface area the material has.

Next, the stability measurements were conducted. Two stability replicates were conducted, and the UV-Vis spectra are shown from one of the runs, Figure **3.12** contains spectra of the nonalkylated COF and the surface modified pyridine COF as a function of time, **Appendix D** contains the rest of the UV-Vis Spectra. From these spectra, half-life

of the material could be calculated by looking at the change in absorbance at 300nm, measurements recorded every minute. The increase in absorbance corresponds to an increase in hydrolyzed monomer concentration, or a decrease in COF-18Å. Using the 0 Order Half Life Equation, the COF-18Å pyridine materials half-life was 35minutes. This is a 3 fold increase in stability over the pristine bare pore material; **Appendix F** contains the rest of the half-life graphs.

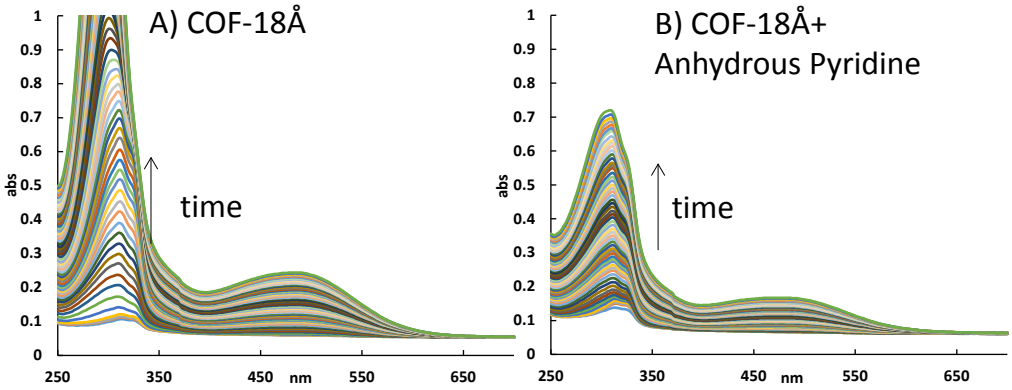

Figure 3.13

A) UV-Vis spectra of COF-18Å from hydrolysis studies, as time progresses two peaks appear, the first peak at 300 nm corresponds to the release of the THB monomer, whereas the absorbance increase at 490 nm corresponds to the autoxidation product of THB. **B)** UV-Vis of COF-18Å+ Anhydrous Pyridine, the pyridine incorporation slows down hydrolysis due to the borons orbitals are occupied, and slows down the nucleophilic water from attacking these orbitals.

Table 3.3 indicates that small changes in structure can have a tremendous impact on properties. The small molecule modification afforded materials with almost a 3 fold increase in stability, with a 2.5 fold decrease in surface area. All the COF-18Å:1P(4VP) materials had a decrease in surface area, with moderate gains in stability, **Fig. 3.13.** The most promising synthetic technique appears to be by simply vortexing the material. This material had the greatest increase in stability, 6 fold, and contained the greatest amount of surface area for these equlmolar materials.

Table 3.3 Summary of Results for Small Molecule Modification

COF	0 order half life	Surface Area(m^2/g)
COF-18Å	13mins+/- .64	715
COF-18Å +Anhydrous Pyridine	35mins+/- 4	275

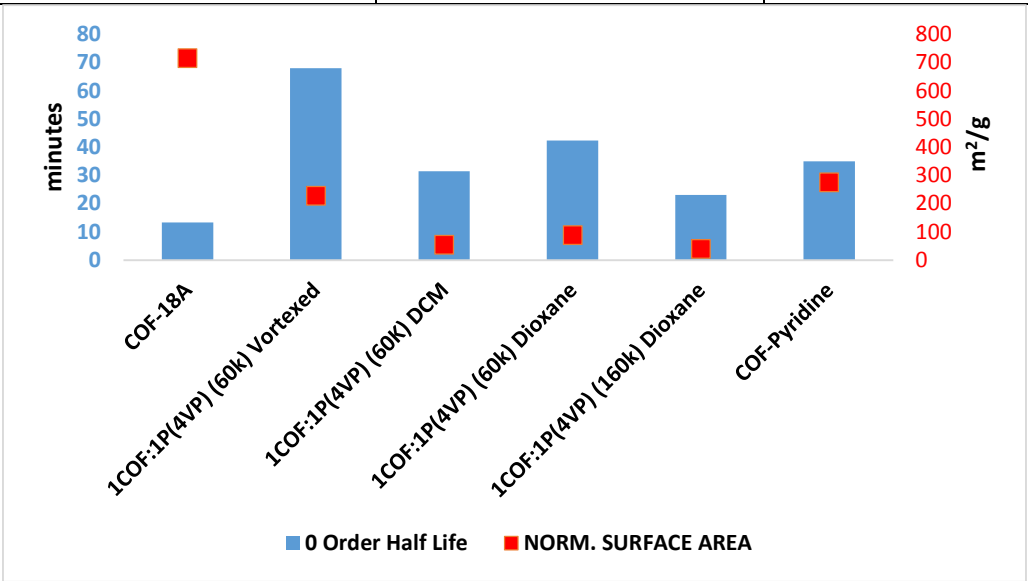

Figure 3.14
Comparison of various synthetic techniques and the impact on properties using an equlmolar ratio of COF and polymer.

Figure 3.14 shows how changing the grafting density impacts properties. The most COF like material contains the worst stability, and greatest surface area. As the amount of COF in these materials decreases, normalized surface area decreases. The 1COF18Å:5(P4VP) material appears to have the greatest surface area, but during the normalization, the uptake was normalized based upon only the COF-18Å weight. As a result, the error in this measurement is possibly quite large. In addition, as the amount of polymer increases the impact on stability is negligible until the material becomes 83%

polymer. From this, one can see that the 2COF18Å:1P4VP, has the optimal surface area and a modest improvement in stability.

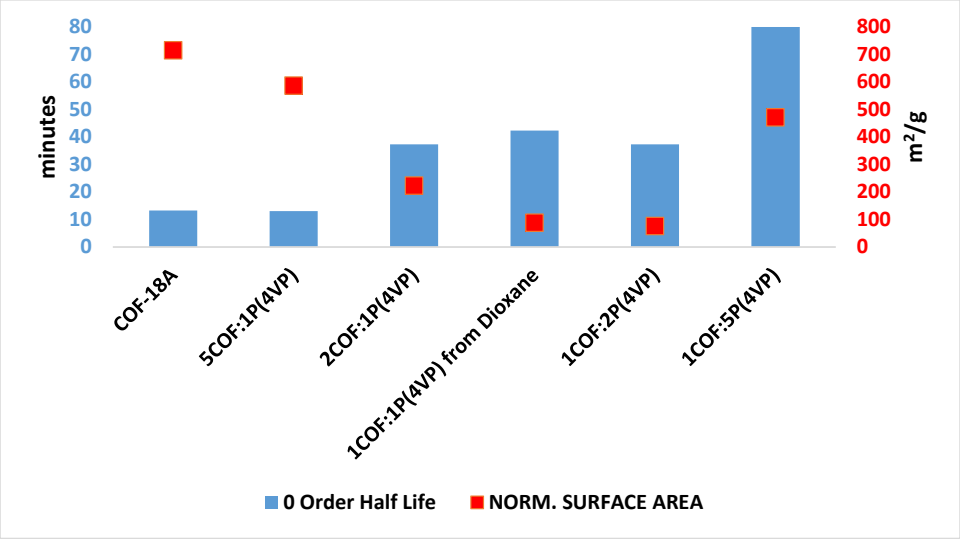

Figure 3.15
Impact of Grafting Density on Properties.

3.4 Conclusion

The incorporation of a small monomer was shown to increase the hydrolytic stability of the COF-18Å, while maintaining the 18Å diameter of COF. The pyridine was not shown to intercalate into the internal layers of the framework, and resulted in the COF-18Å + anhydrous pyridine retaining the typical Type 1 isotherm for these microporous networks. The optimal reaction condition appears to be vortexing the COF-18Å and polymer. Future work could include studying the impact of grafting density on physical mixture

3.5 Experimental

COF-18 Å + Anhydrous Pyridine. COF-18Å (0.100 g, 0.9511 mmol) was placed in a 4 dram vial, and anhydrous pyridine, (0.00712 g, 9.012E-4 mmol) was added. The material was vortexed until the material dispersed evenly, approximately two minutes (large clumps of COF-18Å and pyridine were observed). After mixing, the clumps disappeared and MAS NMR was run. This sample was kept in the rotor. The rest of the material was placed in a vacuum oven <1mm Hg for 18 h to remove excess uncoordinated pyridine.

COF-18 Å + P(4VP) Pyridine Vortexed Mixture. Freshly ground COF-18Å (0.100 g, 0.951 mmol) and freshly ground P(4VP) (0.100g, 0.951 mmol) were placed in a 4 dram vial, and the material was vortexed for 3 minutes. After vortexing the material MAS NMR was run.

General Procedure for the Formation of Face Modified COFs. Various COF-18Å: P(4VP) ratio materials were mixed and heated in dioxane. (Amount of dioxane determined by using 1mL for every 10mg of P(4VP)). Ratio of COF-18Å:P(4VP) varied from 5:1 to 1:5, molecular weight of COF-18 Å repeat unit was 105g/mol. Activated COF-18 Å was used. The solution was refluxed under constant nitrogen flow for 5 h. The reaction mixture was cooled to room temperature and the solvent was removed by distillation. The sample was dried on a vacuum line at ambient temperature overnight. The resulting dried powder was characterized by ^{13}C CP-MAS NMR. After ^{13}C CP-MAS NMR characterization material was ground with mortar and pestle for immediate use.

Gas Adsorption Analysis: Gas adsorption data was collected using a liquid nitrogen bath for nitrogen adsorption isotherm. The dried powder was loaded into a 6mm sample cell (small bulb) and degassed at 250 ºC under high vacuum (<0.001 mm Hg) for 2.5 h.

Hydrolysis Test by Absorbance. Onto a 1 cm x 2 cm rectangle of filter paper, 5 mg of activated and ground COF was carefully weighed. The filter paper was folded in half and the edges were folded closed with tweezers to enclose the COF. The resulting square envelope was placed flat onto the bottom of a 1 cm quartz cuvette with the folds facing the bottom of the cuvette. Immediately prior to the first scan, 3 mL of water was carefully added dropwise to the cuvette over the course of one minute. Absorbance scans were taken without moving the cuvette with a 0.654 mm spacer added to adjust the z factor on a Shimadzu UV-2600 UV-Vis Spectrophotomer. All data were collected at 25 ^{o}C.

3.6 References

1. Du, Y.; Mao, K.; Kamakoti, P.; Ravikovitch, P.; Paur, C.; Cundy,S.; Li, Q.; Calabro, D. Experimental and computational studies of pyridine-assisted post-synthesis modified air stable covalent–organic frameworks. *Chem. Commun.* **2012**, 48, 4606-4608.
2.
3. Du, Y.; Mao, K.; Kamakoti, P.; Wooler, B.; Cundy, S.; Li, Q.; Ravikovitch, P.; Calabro, D. The effects of pyridine on the structure of B-COFs and the underlying mechanism *J. Mater. Chem. A***, 2013**, *1*, 13171-13178.

4. Weiss W. J.; Bryce L. D.; A Solid-State ^{11}B NMR and Computational Study of Boron Electric Field Gradient and Chemical Shift Tensors in Boronic Acids and Boronic Esters. *J. Phys. Chem. A.* **2010**, *114*, 5119-5131.

CHAPTER 4: Synthesis of Edge Modified Covalent Organic Framework

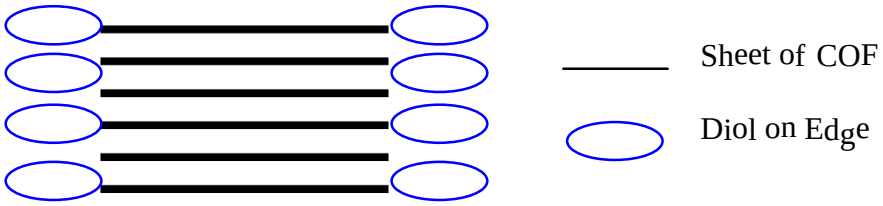

Figure 4.1
Cartoon to elucidate where bonding occurs on edge modified material.

4.1 Overview:

This section pertains to the functionalization of the COF-18Å surface with boronic acid derivatives. During the polymerization in which the COF-18Å framework is synthesized, an excess amount of diol is used to ensure that the COF is capped with diols. These terminal diols, highlighted in **Figure 4.1**, decorating COF-18Ås surface were functionalized using a plethora of materials containing a boronic acid handle, to form a second boronate ester extended off of the framework. First, attention was focused on attempting to modify the exterior using small molecules with unique spectroscopy properties. However, due to the size of the COF-18Å with respect to a small molecule, this task was difficult to quantify using spectroscopy.

As a result, attention shifted from small molecules to synthesizing a modified RAFT agent containing a boronic acid.[1] This was troublesome as well due to the fact that each polymer chain contained only one boronic acid. In order to increase the valency, boronic acid handles were introduced into the repeat unit of the polymers. By increasing

the number of boronic acids, modification of the exposed diols was possible, resulting in material with unique properties.[2,3]

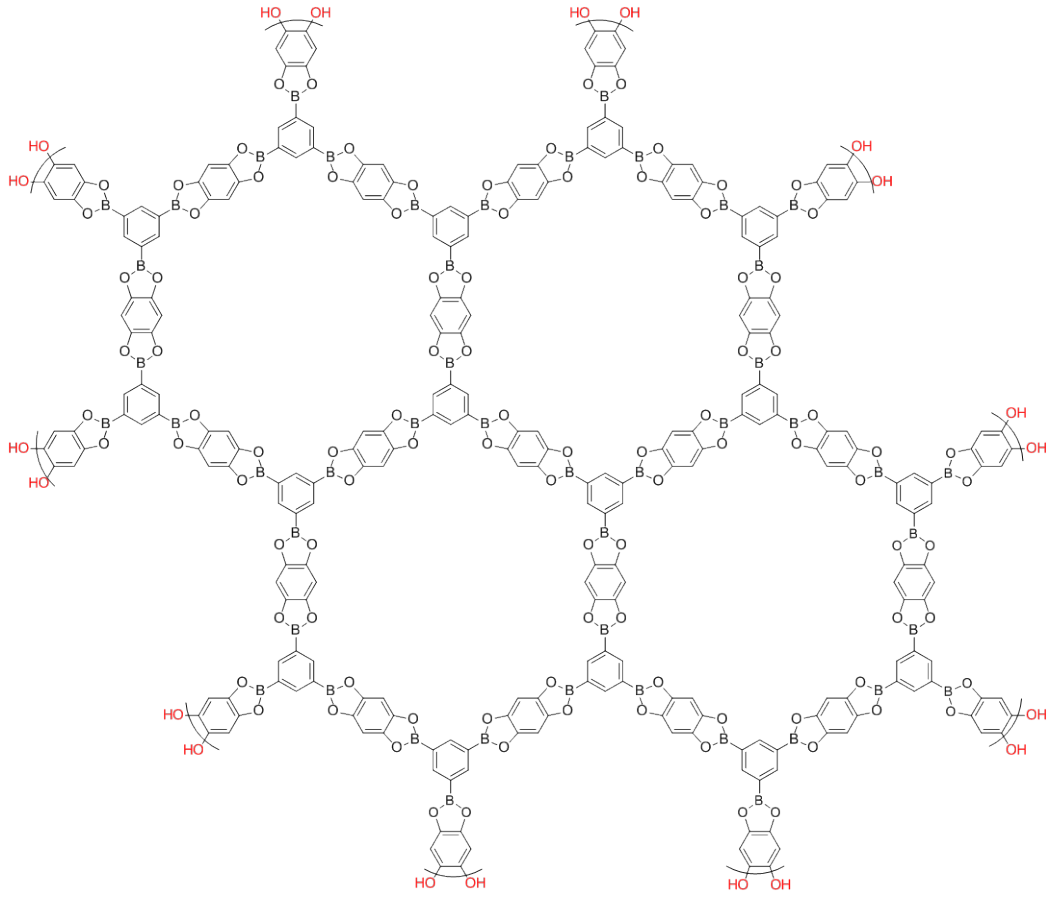

Figure 4.2
The basic structure of a COF-18 Å. Post Polymerization Modification occurred off of the end group diols.

4.2 Results and Discussion

The first attempt at synthesizing edge modified materials was to take a small molecule, 3-(tert-butyldimethylsilyloxy)phenylboronic and react it with the COF-18Å. After heating the materials to reflux, the insoluble COF material was obtained by filtration, where the soluble boronic acid was rinsed away, leaving behind only the modified COF-18 Å and unmodified COF-18 Å.

The ^{13}C CP_MAS spectrum **Figure 4.2A** contains spinning sideband suppression, and this sacrificed the sensitivity of the experiment. This can be seen in **Figure 4.2B**, where only COF and solvent remains.

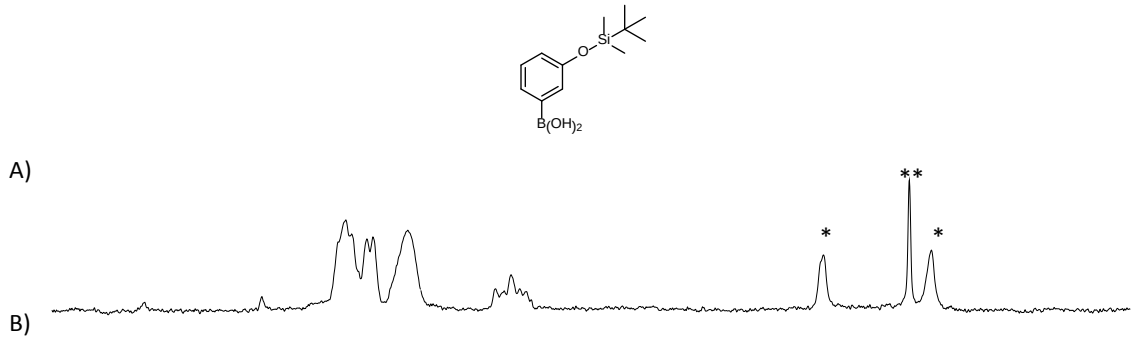

Figure 4.3

^{13}C CP-MAS NMR of **A)** 3-(tert-butyldimethylsilyloxy)phenylboronic acid, multiple resonances due to semi anhydride formation. **B)** COF-18Å + TBDMS-$B(OH)_2$.* Represents residual THF trapped in the pores, and ** represents CH_2Cl_2 in the pore.

^{13}C CP-MAS NMR did not show any evidence of modification, but perhaps the modification level was too low to detect. As a result, solid state silicon NMR was implemented with the expectation of seeing the silicon resonance after attachment. However, as **Figure 4.3** shows, after the reaction either the edge modification failed, or the reaction worked but the modification worked and was below the limit of detection of the NMR. As a result, attention shifted to using polymers containing boronic acids.

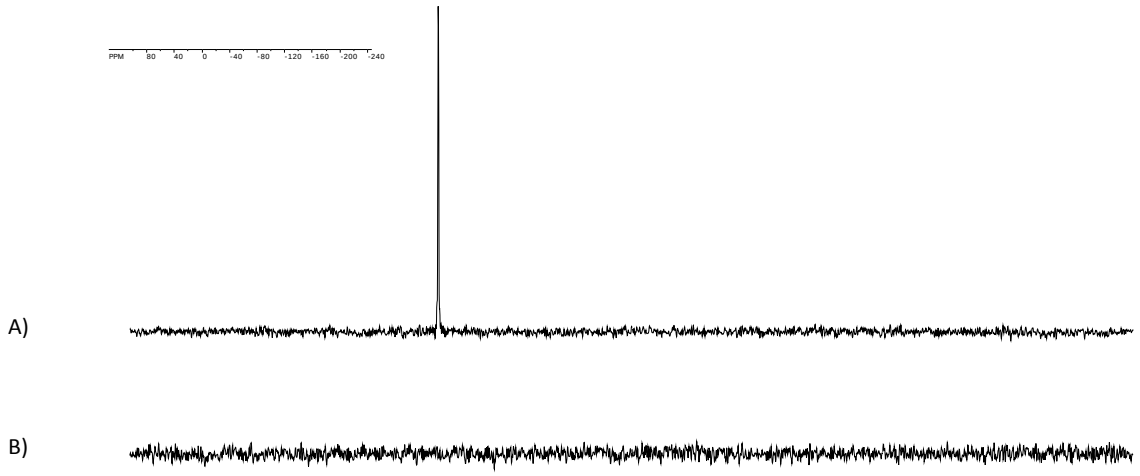

Figure 4.**4**
^{29}Si MAS NMR for starting material A) TBDMS-B(OH)$_2$. B) COF-18A+ TBDMS-B(OR)$_2$ after workup.

The next approach was to use a RAFT agent containing a boronic acid handle, this would then be able to be attached to the diol resulting in a second boronate ester bond. This reaction was monitored by Differential Scanning Calorimetry(DSC). The approach was to react the COF-18 Å and the styrene polymer containing a boronic acid end group. After the reaction, the material was rinsed with excess THF, until the visible yellow solution went clear. After the workup, the material was dried and DSC was implemented, with the expectation of seeing a T_g from the polystyrene. In addition, this T_g was thought to be at a higher temperature due to the decreased chain mobility. However, as **Figure 4.4B s**hows that the isolated material does not contain a T_g, or it is there but below the limit of detection.

This led us to believe that in order to increase the likelihood of the boronic acid and diol reacting, the number of mols of boronic acids needed to be increased. This

increase could either be from introducing more polystyrene terminated boronic acid chains, or by introducing the same number of chains, but with pendant chain boronic acid moieties.Even if more boronic acid RAFT agents were introduced the chances of having the diols finding am end group were low, as each chain only contains a single boronic acid. As a result, the latter was pursued, where every repeat unit contains a boronic acid handle that can potentially bond to the diol end groups from the COF.

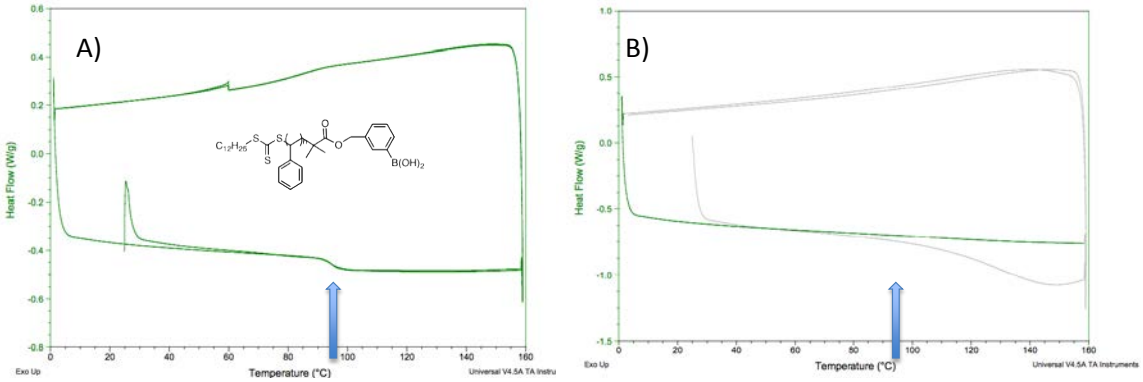

Figure 4.5
A) DSC of PS-terminated $B(OH)_2$ starting material. **B)** DSC of COF18Å + PS-$B(OH)_2$ after workup.

Three methods for preparing boronic acid pendant chain materials are outlined below. The first method **Figure 4.5A)** was a direct way to obtain this material, however due to the fact that boronic acids can form a trimer and become an anhydride, the product gelled, most likely due to formation of anhydride which would result in crosslinking of the boronic acid polymer.. Yakel's group made a boronic aicd polymer using the polymer shown in **Figure 4.5 B)**, if n-buLi and triisopropyl borate are used, the material precipitates out of THF [4]. As a result, the method which successfully gave a boronic acid polymer is the reaction scheme shown in **Figure 4.5C.**. RAFT polymerization of the 3-ABA was first published by Dr. Sumerlin's group, and afforded a boronic acid

containing polymer via RAFT polymerization.[2] As a result, the literature procedure to form this this material was followed.

In order to obtain molecular weight and PDI, the material was esterified with neopentyl glycol and distilling from toluene thrice with a molecular weight around 10k. The material was esterified to prevent the boronic acid polymer from binding to the GPC column.[1] The transformation of boronic acid polymer to boronate ester polymer allowed for facile characterization. After obtaining, this material attention shifted to modifying the COF-18 Å surface. Several methods were considered, such as synthesizing the COF-18 Å, and then doing a post polymerization modification of the surface, with the polymer. All of the previous methods described for the COF modifications were carried out this way without affording a modified framework.

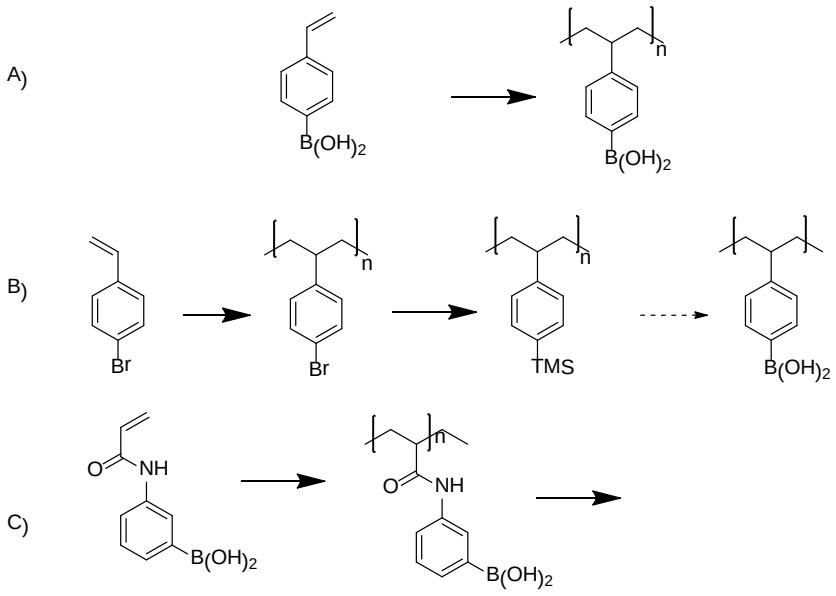

Figure 4.**6**
Generic synthetic routes to obtain pendent chain boronic acid polymers.

Previously in Chapter 2, a microwave assisted polymerization of THB and BTBA to afford a crystalline covalent organic framework in one hour was discussed. As a result, this synthetic technique was implemented with an in-situ one pot synthesis of edge modified COF, as shown in **Figure 4.6**. To do this, THB and BTBA were reacted for one hour. After the reaction stopped, the polymer was added via a syringe to the vessel, and reacted for an additional hour. This material was then rinsed with THF, until the mother liquor fractions went colorless as color is indicative of the polymer from the RAFT agent. It is important to note here that the activation of COF-18 Å by the microwave route, did not require the three day rinsing that the traditional COF-18 Å requires. The PXRD from **Chapter 2** was of the crude reaction after filtration. Rinsing with large quantities allows for the removal of the small molecule by products.

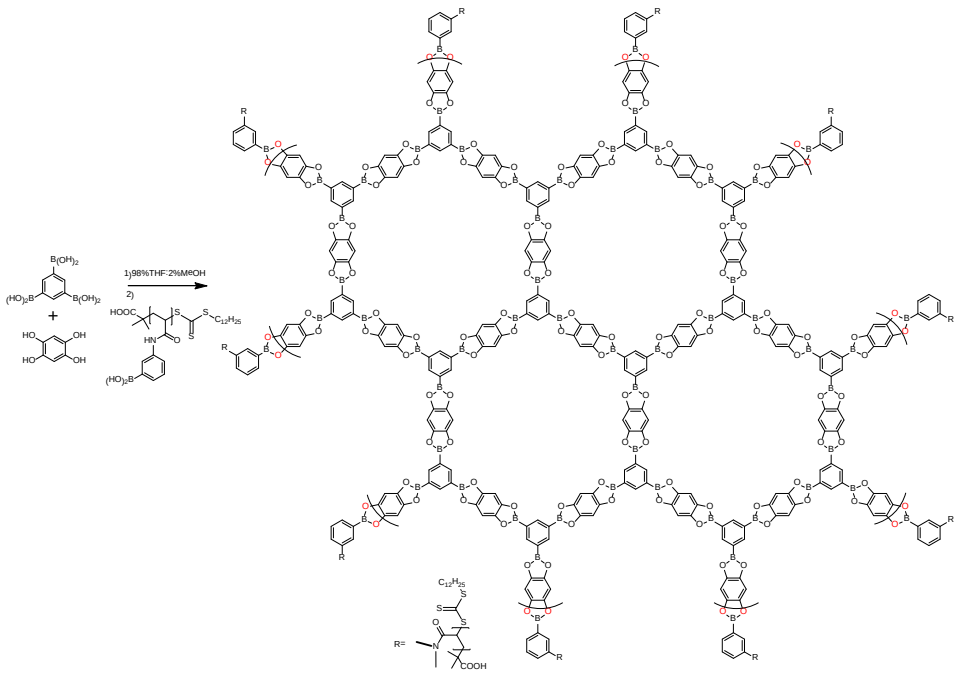

Figure 4.7
Edge Modified COF-18Å Synthetic Scheme.

4.2.1 Characterization of Edge Modified COF

The COF-18 Å was characterized using ^{13}C CP-MAS NMR, PXRD, gas adsorption and stability measurments. ^{11} B NMR was avoided because the new boronate ester bond was also sp^2 hybridized and would overlap with the internal and external sp^2 resonances. The NMR in **Figure 4.7** shows that the polymer is present in the COF-18 Å, side ban supression was used and as a result, the sensitivity of this experiment decreased. Poly acrylomidophenyl boronic acid P(ABA) has a carbonyl resonance around 170 PPM, and the aliphatic carbons have a resonance around 40 PPM. In addition, the relative heights of the COF-18Å and P(ABA) are sensitive to crosspolarization, and do not indicate amount of polymer present, this this measurement is purely qualitative. Knowing that the material contained a polymer and COF, attention focused on determining if the material was bound or not.

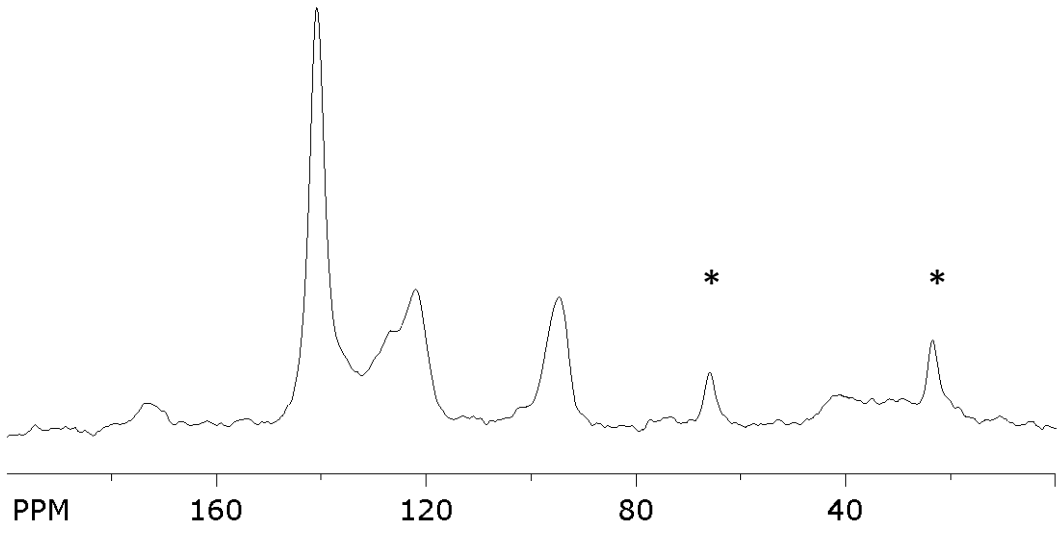

Figure 4.8
^{13}C CP-MAS NMR of Edge Modified COF-18Å, sample contains THF denoted with*.

To get a further understanding of structure, PXRD was used on a zero background slide. The material appears to look different than the COF-18 Å, (see Chapter 2 for a full description on COF-18 Å PXRD). COF-18 Å generally has 5 peaks associated with it. The low degree 2θ peak is present, which is generally associated with the 18 Å center-center distance, (100), but greatly diminished, The overall crystallinity determined by the peak width is also much lower. This is expected because the amorphous polymer was able to react with the COF-18 Å, and perturb the crystal structure, **Figure 4.8.** After understanding the characterization of the materials, we decided to test this novel COF-18 Å with respect to stability and gas adsorption. Future work includes determination of the amount of polymer present in the framework.

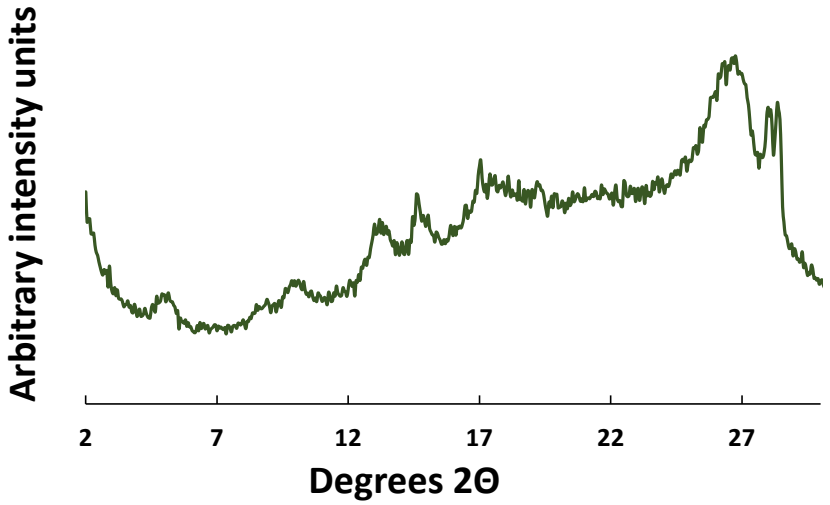

Figure 4.9
PXRD of the newly formed Edge Modified COF-18Å.

4.3 Bulk Properties

The first bulk property investigated was whether the polymer improved the COF-18Å stability. As previously described in Chapter 3, UV-Vis was implemented to

monitor the release of THB at the 300 nm wavelength. Due to the low solubility of the P(ABA) in water, the polymer did not interfere with these measurements. A control UV-Vis experiment of just the P(ABA)s was studied, and the absorbance was under 0.1 after one hour. The incorporation of the polymer had a significant impact on stability, **Appendix E** contains the raw UV-Vis data for the edge modified COF. From these spectra, one was able to follow the release of THB, which was shown in **Figure 4.9**. This figure demonstrates that the rate of release of monomer is greatly retarded by a small amount of polymer. This polymer, is able to prevent the water from coordinating with the COF-18 Å s boronate esters.

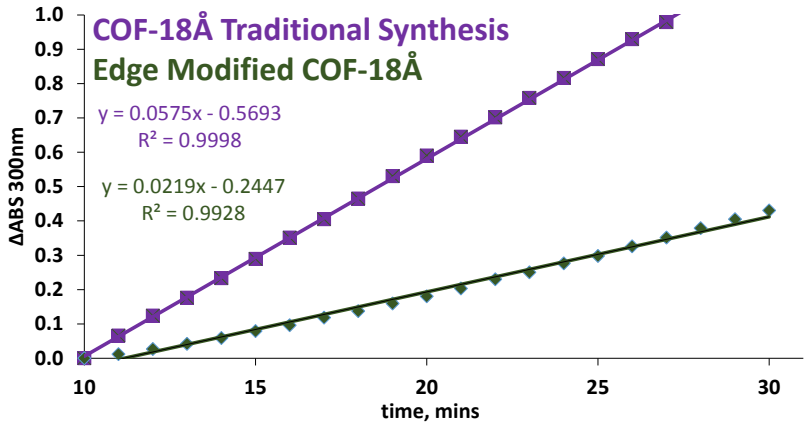

Figure 4.**10**
Relative stability of COF-18 Å vs edge modified material.

Lastly, Gas Adsorption measurements were conducted on these materials, to see if these frameworks maintained a Type 1 isotherm, indicative of COF-18Å. The microwave COF-Fig **4.10A**) and microwave edge modified COF-18Å, **Fig 4.10B** both contain this Type 1 isotherm indicative of a micro porous network.

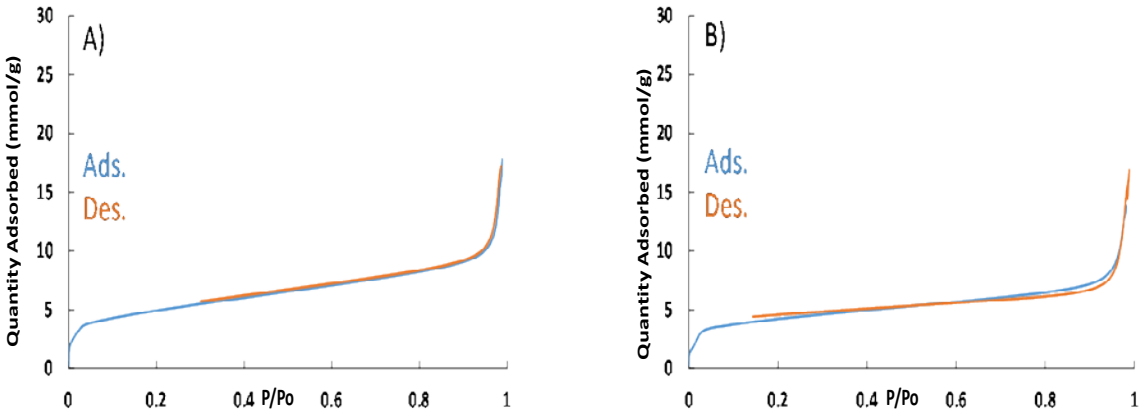

Figure 4.11
A) Microwave Synthesis of COF-18Å, adsorption and desorption isotherm. **B)** Microwave COF-18Å, + PAMPBA adsorption and desorption isotherm.

4.4 Conclusion

The attachment of polymer to a COF-18Å allows for a more stable network, with about a 4 fold increase in stability, 17 minutes. The inclusion of the polymer did not impact the materials ability to adsorb nitrogen gas, type-1 isotherm. Surface area was not calculated because the grafting density is unknown, which will make the material appear to have a significantly lower surface area than in reality.

Rinsing of the microwave COF-18Å, afforded activated material. This strenuous rinsing was implemented for the edge modified microwave COF preparation and removed any unbound small molecule byproducts. If small molecules were present ^{13}C CP-MAS NMR sharp signals would be present, however, the resonances are very broad indicative of polymers. In addition, the PXRD powder pattern is substantially different than the pristine COF-18Å. This change is indicative of an edge modification, as the crystal lattice has changed.

Future work will go into elucidating how much polymer is bound, and what the appropriate grafting density, and molecular weight are required to give the material with the highest stability, while maintaining the integral 18Å diameter.

4.5 Experimental

Edge Modified COF with TBDMS-B(OH)$_2$. 3-(tert-butyldimethylsilyl)phenyl boronic acid (0.150 g, 0.595 mmol) dissolved in DCM (2 mL) was added to a flask containing COF-18Å (0.052 g, 0.0047 mmol)[14] material was heated to reflux overnight. Material was rinsed with 500mL dry DCM, UV-Vis on aliquots of mother liquor waited for absorbance to reach 0.001. The material was collected and dried overnight. This afforded the edge modified COF with TBDMS-B(OH)$_2$ (0.080 g) as a powder.

Edge Modified COF with PS-B(OH)$_2$

A 12000D polystyrene end functionalized boronic acid polymer (0.0329 g, 0.002741 mmol) and COF-18Å (0.041 g, 0177 mmol) were heated to reflux in THF (5 mL) for a week, under nitrogen. Solvent replenished to original amount each day. Solution filtered and washed with copious amounts of THF. Rinses with THF occurred until unreacted polystyrene was extracted, determined by rinsing extract with methanol. The material was dried under reduced pressure overnight. This workup afforded the edge modified COF with PS-B(OH)$_2$ (0.018 g) as a powder.

[14] M_w of COF-18Å 11063 D.

Synthesis of 3-acrylamidophenylboronic acid (APBA). 3-aminiophenyl boronic acid (9.97 g, 73.27 mmol) and sodium bicarbonate (13.6 g, 162.1 mmol) were dissolved in a round bottom flask containing a mixture of THF (100 mL) and water (100 mL). Acryloyl chloride (16.3 g, 179 mmol) was added dropwise to the flask at 0-5 ºC. The solution was stirred overnight, ethanol was added to facilitate distillation of H_2O and THF. A solid crude product was obtained and stirred in ethyl acetate until the material dissolved. After the material dissolved, the ethyl acetate layer was washed with water (50 mL), saturated sodium bicarbonate solution (50 mL), water (50 mL), and brine (50 mL). The ethyl acetate layer was concentrated under reduced pressure. The monomer was purified by recrystallization from hot water (×3). The workup provided APBA (8.38g, 60%) as an orange solid.

^{1}H NMR (300 MHz, DMSO): δ 10.1 (s, 1 H) 8.1 (s, 2 H,) 7.9 (s, 1 H) 7.84-7.80 (d, 1H) 7.61-7.59 (d, 1H) 7.41-7.39 (d, 1H) 7.22-7.20 (t, 1H) 6.4-6.30 (dd 1H) 5.75-5.70(dd, 1H)

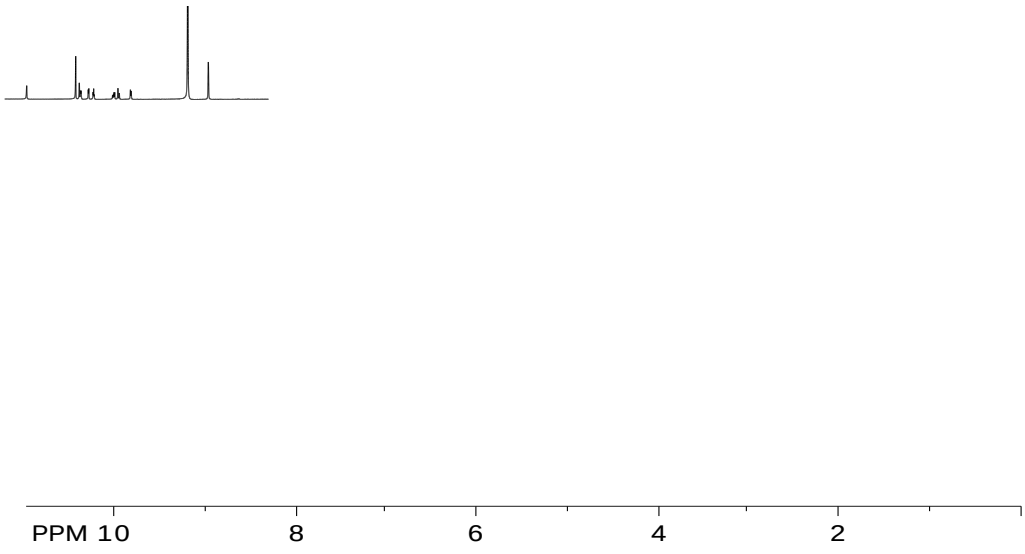

Figure 4.12
^{1}H NMR of Monomer.

RAFT Polymerization of (3-acrylamidophenyl) boronic acid

APBA (6 g, 31.41 mmol), DMP (0.120 g, 0.329 mmol), 2,2′-azobis(isobutyronitrile) (AIBN) (7.0 mg, 0.042 mmol), DMF/water mixture (30 mL 95/5 vol.-%) were sealed in a 20 mL vial ([APBA]/[CTA]/[AIBN]= 95/1/0.1). The solution was deoxygenated by sparging with nitrogen for 40 min and then placed in a preheated reaction block at 70 °C for 5h. The final polymer was isolated by removing DMF/water under vacuum, dissolving in methanol, and precipitating into diethyl ether.

^{1}H NMR (300 MHz, MeOD):

Figure 4.13
^{1}H NMR of Polymer.

4.6 References

1. Sudershan, D., P.; Gondi, S.; Roy, D.; Sumerlin, B. Boronic Acid Terminated Polymers: Synthesis by RAFT and Subsequent Dynamic Covalent Self-Assembly. *Macromolecules.* **2009**, *42*, 5614-5621.

2. Cambre, J.; Roy, D.; Gondi, R.; Sumerlin B. Facile Strategy to Well-Defined Water-Soluble Boronic Acid (Co)polymers. *J. Am. Chem. Soc.* **2007**, *129*, 10348-10349.

3. Cambre, N. J.; Roy, D.; Sumerlin, S. B.; Tuning the sugar-response of boronic acid block copolymers. *J. Polym. Sci., Part A: Polym. Chem.*, **2012** *50,* 3373-3382.
4. Qin, Y.; Cheng, G.; Achara, O.; Parab, K.; Jakle, F. A New Route to Organoboron Polymers via Highly Selective Polymer Modification Reactions. *Macromolecules*. ***2004***, 37, 7123-7131.

Bibliography

Cambre, J.; Roy, D.; Gondi, R.; Sumerlin B. Facile Strategy to Well-Defined Water-Soluble Boronic Acid (Co)polymers. J. Am. Chem. Soc. **2007**, 129, 10348-10349.

Cambre, N. J.; Roy, D.; Sumerlin, S. B.; Tuning the Sugar-Response of Boronic Acid Block Copolymers. *J. Polym. Sci., Part A: Polym. Chem.*, **2012** *50*, 3373-3382.

Campbell, N. L.; Clowes, R.; Ritchie, L. K.; Cooper, A. I. Rapid Microwave Synthesis and Purification of Porous Covalent Organic Frameworks. *Chem. Mater* **2009**, 21, 204-206.

Christinat, N.; Croiser, E.; Scopelliti, R.; Cascella, M.; Rothlisberger, U.; Severin, K. Formation of Boronate Ester Polymers with Efficient Intrastrand Charge Transfer Transitions by Three-Component Reactions. *Eur. J. Inorg. Chem.* **2007**, 5177-5181.

Cote, A. P.; Benin, A. I.; Ockwig, N. W.; O'Keeffe M.; Matzger, A. J.; Yaghi O., M.; Porous, Crystalline, Covalent Organic Frameworks. *Science* **2005**, *310*, 1166-1170

Du, Y.; Mao, K.; Kamakoti, P.; Ravikovitch, P.; Paur, C.; Cundy,S.; Li, Q.; Calabro, D. Experimental and Computational Studies of Pyridine-Assisted Post-Synthesis Modified Air Stable Covalent–Organic Frameworks. *Chem. Commun.* **2012**, 48, 4606-4608.

Du, Y.; Mao, K.; Kamakoti, P.; Wooler, B.; Cundy, S.; Li, Q.; Ravikovitch, P.; Calabro, D. The Effects of Pyridine on the Structure of B-COFs and the Underlying Mechanism *J. Mater. Chem. A*, **2013**, *1*, 13171-13178.

Farha, K.O.; Yazaydin O.; Eryazici, I.; Malliakas, D. C.; Hauser, G. B.; Kanatzidis, G. M.; Nguyen, T. S.; Snurr, Q. R.; Hupp, T. J. De novo Synthesis of a Metal-Organic Framework Material Featuring Ultrahigh Surface Area an Gas Storage Capacities *Nature Chemistry* **2010**, *2 944-948.*

Kandambeth, S.; Mallick, A.; Lukose, B.; Mane, V., M.; Heine, T.; Banerjee, R. Construction of Crystalline 2D Covalent Organic Frameworks with Remarkable Chemical (Acid/Base) Stability via a Combined Reversible and Irreversible Route. *J. Am. Chem. Soc.*, **2012**, *134*, 19524–19527.

Kandambeth, S.; Shinde, B., D.; Manas, K.; Panda, L., B.; Lukose, B.; Heine, T.; Banerjee, R Enhancement of Chemical Stability and Crystallinity in Porphyrin-Containing Covalent Organic Frameworks by Intramolecular Hydrogen Bonds. *Angew. Chem. Int. Ed*. **2013**, 52, 13052–13056.

Lanni, M. L.; Tilford, R. W.; Bharathy, M.; Lavigne, J. J. M Enhanced Hydrolytic Stability of Self-Assembling Alkylated Two-Dimensional Covalent Organic Frameworks. *J. AM. Chem. Soc.* **2011**, 133, 13975-13983.

Milwar, A.; Yaghi, O. Metal-Organic Frameworks with Exceptionally High Capacity for Storage of Cabon Dioxide at Room Temperature. *J. Am. Chem. Soc.* **2005**, *127*, 17998-17999.

Moad, G.; Rizzardo, E.; Thang, S.H. Living Free-Radical Polymerization by Reversible Addition-Fragmentation Chain Transfer: The RAFT Process. *Macromolecules.* **1998**, *31*, 5559-5562.

Qin, Y.; Cheng, G.; Achara, O.; Parab, K.; Jakle, F. A New Route to Organoboron Polymers via Highly Selective Polymer Modification Reactions. *Macromolecules*. ***2004***, 37, 7123-7131.
Qin, Y.; Cui, C.; Jakle F. Silylated Initiators for the Efficient Preparation of Borane-End-Functionalized Polymers via ATRP. *Macromolecules* **2007,** *40*, 1413-1420.

Qin, Y.l;, Sukul, V.; Pagakos, D.; Jakle F.; Preparation of Organoboron Block Copolymers via ATRP of Silicon and Boron-Functionalized Monomers. *Macromolecules.* **2005** *38*, 8987-8990

Rambo, M. B.; Lavigne, J. J. Defining Self-Assembling Linear Oligo(dioxaborole)s. *Chem. Mater.* **2007,** *19*, 3732-3739.

Saha, D.; Deng, S. Structural Stability of Metal Organic Framework MOF-177. *J. Phys. Chem. Lett.* **2010**, *1*, 73-78.

Sudershan, D., P.; Gondi, S.; Roy, D.; Sumerlin, B. Boronic Acid Terminated Polymers: Synthesis by RAFT and Subsequent Dynamic Covalent Self-Assembly. *Macromolecules.* **2009**, *42*, 5614-5621.

Sudik, A.; Ockwig, N.; Cote, A.; Kim, J.; Yaghi, O. Design, Synthesis, Strcture, and Gas (N2, Ar, CO2, CH4 and H2) Sorption Properties of Porous Metalorganic Tetrahedral and Hetrocuboidal Polyhedra. *J. Am. Chem. Soc.* **2005**, *127, 7110-7118.*

Tilford, R. W.; Gemmill, W. R.; zur-Loye, H.-C.; Lavigne, J. J. Facile Synthesis of a Highly Crystalline, Covalently Linked Porous Boronate Network. *Chem. Mater* **2006**, 18, 5296-5301.

Tilford, R. W.; Mugavero, J. S.; Pellechia, J. P.; Lavigne, J. J. Tailoring Microporosity in Covalent Organic Frameworks. *Adv. Mater.* **2008**, 20, 2741-2746.

Wang, J. S.; Matyjaszewski, K. Controlled/"Living" Radical Polymerization. Atom Transfer Radical Polymerization in the Presence of Transition-metal Complexes. *J. Am. Chem. Soc.* **1995**, *117*, 5614-5615.

Weiss W. J.; Bryce L. D.; A Solid-State ^{11}B NMR and Computational Study of Boron Electric Field Gradient and Chemical Shift Tensors in Boronic Acids and Boronic Esters. *J. Phys. Chem. A.* **2010**, *114*, 5119-5131.

Yaghi O., M.; O'Keeffe M.; Ockwig N., W.; Chae H., K.; Eddaoudi M.; Kim J. Reticular Synthesis and The Design of New Materials. *Nature* **2003**, *423*, 705-714.

Appendix A – ^{11}B NMR

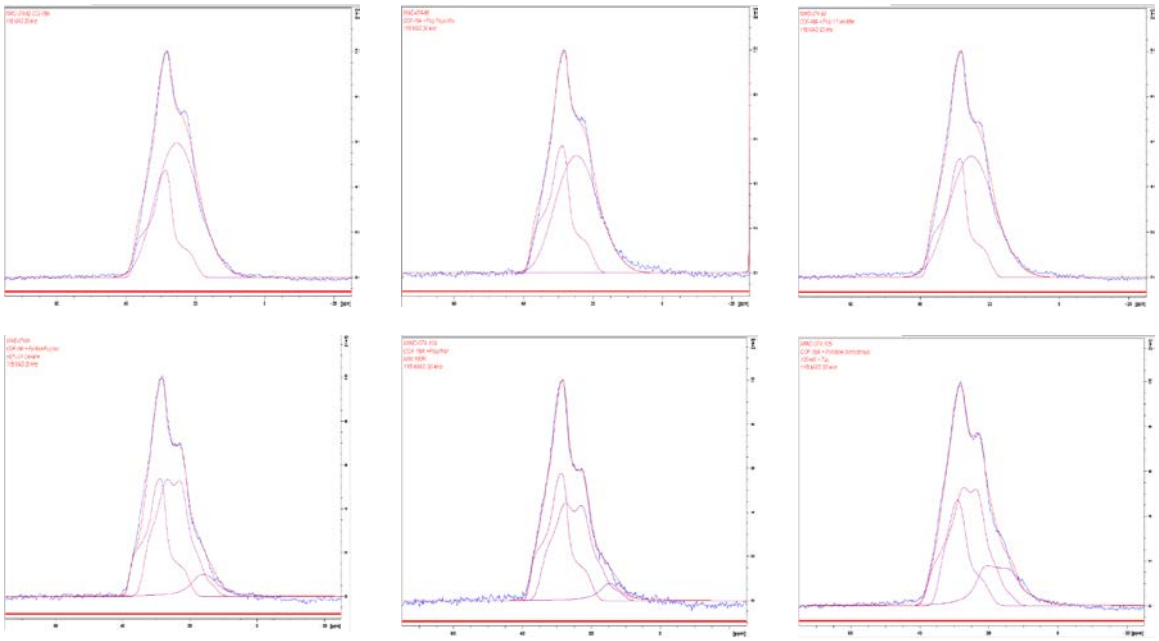

Figure A.1
^{11}B MAS NMR of physical mixture COF

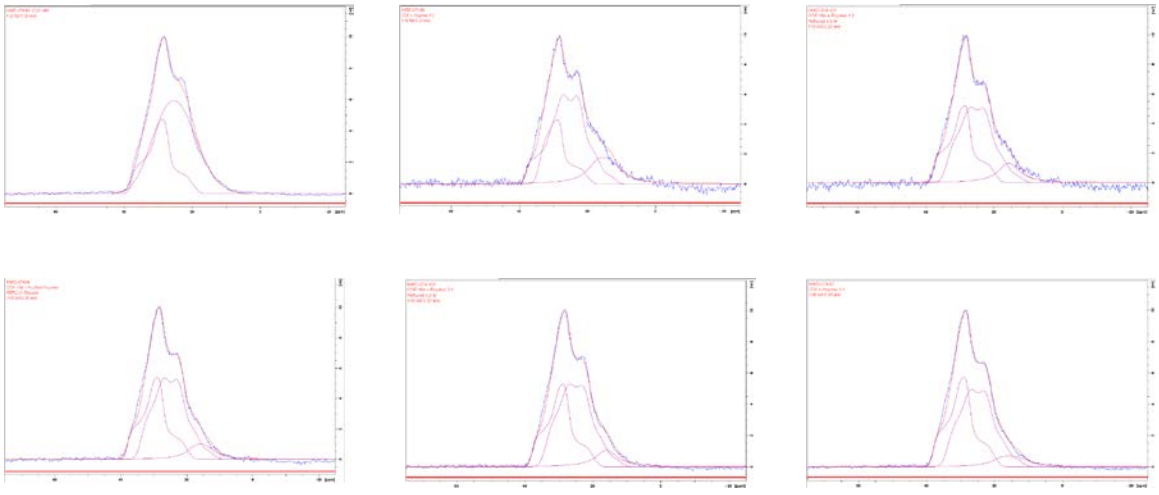

Figure A.2
^{11}B MAS NMR of various face modified COF

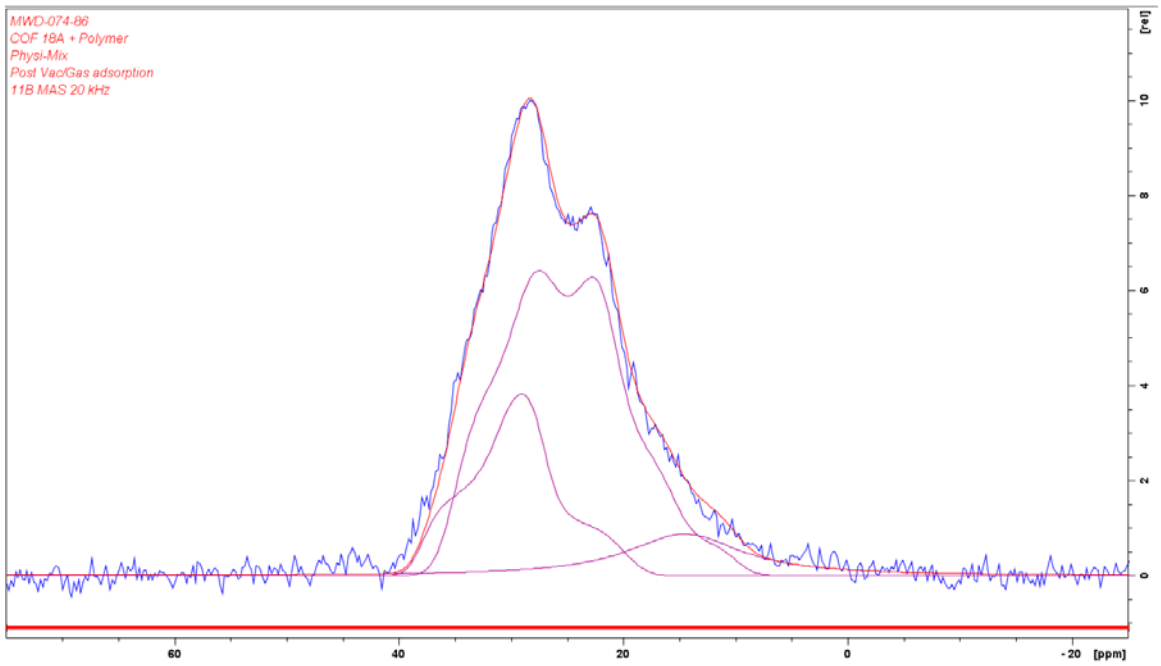

Figure A.3

^{11}B MAS NMR of Physical Mixture COF after gas adsorption

Appendix B – Fit Logs

COF-18A
11B MAS 20 kHz

SITES	1	2	
Iy	448274.6*		610531.6*
delta(iso)	38.183*	34.852*	
CQ(Quad)		2400	2300
nuQ(Quad)		1200	1150
eta(Quad)		1.25	1.6
LB	0	0	
GB	315.7169*		1283.9833*
Integral	100	221.57	

Starting Overlap(%) 88.43819032927023
Overlap(%) 88.49168268654752

Stirred Physical mixture

SITES	1	2	
Iy	326268.1*		332728*
delta(iso)	38.162*	34.67*	
CQ(Quad)		2400	2300
nuQ(Quad)		1200	1150
eta(Quad)		1.25	1.6
LB	0	0	
GB	314.7192*		1549.4014*
Integral	100	177.08	

SIMPLEX Optimization Started
Starting Overlap(%) 86.21435902580042

Vortexed Physical Mixture

SITES	1	2	
Iy	298826.7*		266612.9*
delta(iso)	38.0	33.909*	
CQ(Quad)		2400	2300
nuQ(Quad)		1200	1150
eta(Quad)		1.25	1.6
LB	0	0	
GB	351.1654*		1391.2883*
Integral	100	147.56	

Figure B.1
Fit Logs of pristine COF and physical mixture COF.

COF + Polymer 5:1

SITES	1	2	3	
Iy	472096.3*		405098.4*	56428.3*
delta(iso)	38.477*	34.739*	20.801*	
CQ(Quad)		2400	2300	2338*
nuQ(Quad)		1200	1150	1169
eta(Quad)		1.25	1.6	0.0*
LB	0	0	1153.9223*	
GB	339.2711*		516.1166*	0
Integral	100	122.38	20.1	

SIMPLEX Optimization Started
Starting Overlap(%)87.05873286669312
Overlap(%) 87.21529689172931

COF + Polymer 2:1

SITES	1	2	3	
Iy	296095.8*		344463.9*	70806.9*
delta(iso)	38.351*	34.863*	16.338*	
CQ(Quad)		2400	2300	724*
nuQ(Quad)		1200	1150	362
eta(Quad)		1.25	1.6	0.0*
LB	0	0	891.5277*	
GB	380.3237*		534.3394*	0
Integral	13869811.21		22832783.75	3100634.14

SIMPLEX Optimization Started
Starting Overlap(%)86.34206217988255

COF + Polymer 1:1

SITES	1	2	3	
Iy	287337.7*		286058.6*	55357.2*
delta(iso)	38.409*	34.782*	20.205*	
CQ(Quad)		2400	2300	2050*
nuQ(Quad)		1200	1150	1025
eta(Quad)		1.25	1.6	0.0*
LB	0	0	978.4684*	
GB	346.7881*		498.6084*	0
Integral	100	141.25	26.3	

SIMPLEX Optimization Started
Starting Overlap(%)84.67979788314142

COF-18A + Polymer 1:2

SITES	1	2	3	
Iy	93309.4*	117910.8*		25695.9*
delta(iso)	38.212*	34.946*	16.419*	
CQ(Quad)		2400	2300	693*
nuQ(Quad)		1200	1150	346
eta(Quad)		1.25	1.6	0.0*
LB	0	0	1125.0726*	
GB	358.6347*		510.1922*	0
Integral	100	179.13	32.51	

SIMPLEX Optimization Started
Starting Overlap(%)74.99009646009549

MWD-074-87
COF + Polymer 1:5

SITES	1	2	3	
Iy	98615.3*	137161.5*		40840.9*
delta(iso)	38.436*	34.869*	19.56*	
CQ(Quad)		2400	2300	2108*
nuQ(Quad)		1200	1150	1054
eta(Quad)		1.25	1.6	0.0*
LB	0	0	1182.9593*	
GB	284.4091*		459.2855*	0
Integral	100	199.34	66.44	

SIMPLEX Optimization Started
Starting Overlap(%)76.0484478433414

Figure B.2
Fit Logs of Face Modified COF various grafting densities.

Appendix C- PXRD

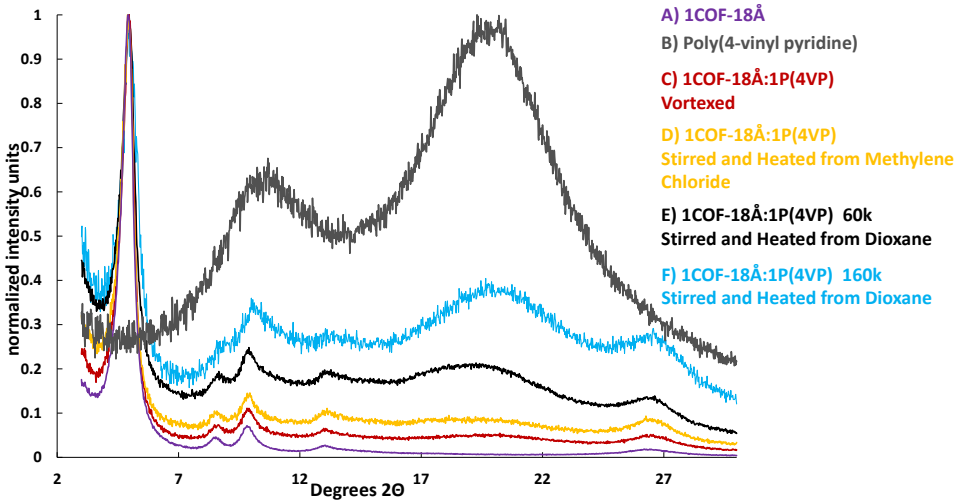

Figure C.1

PXRD of physical mixture COFs

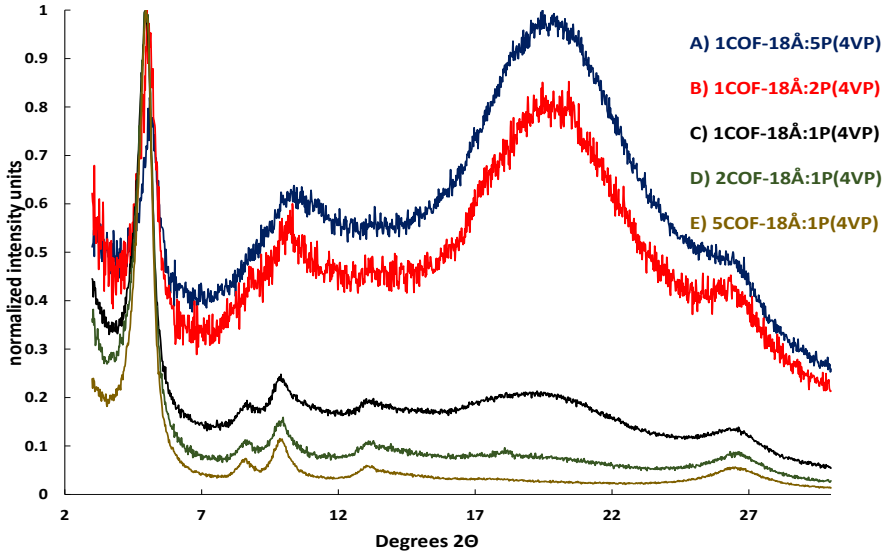

Figure C.2

PXRD of Face Modified COFs various grafting densities.

Appendix D – Nitrogen Isotherms

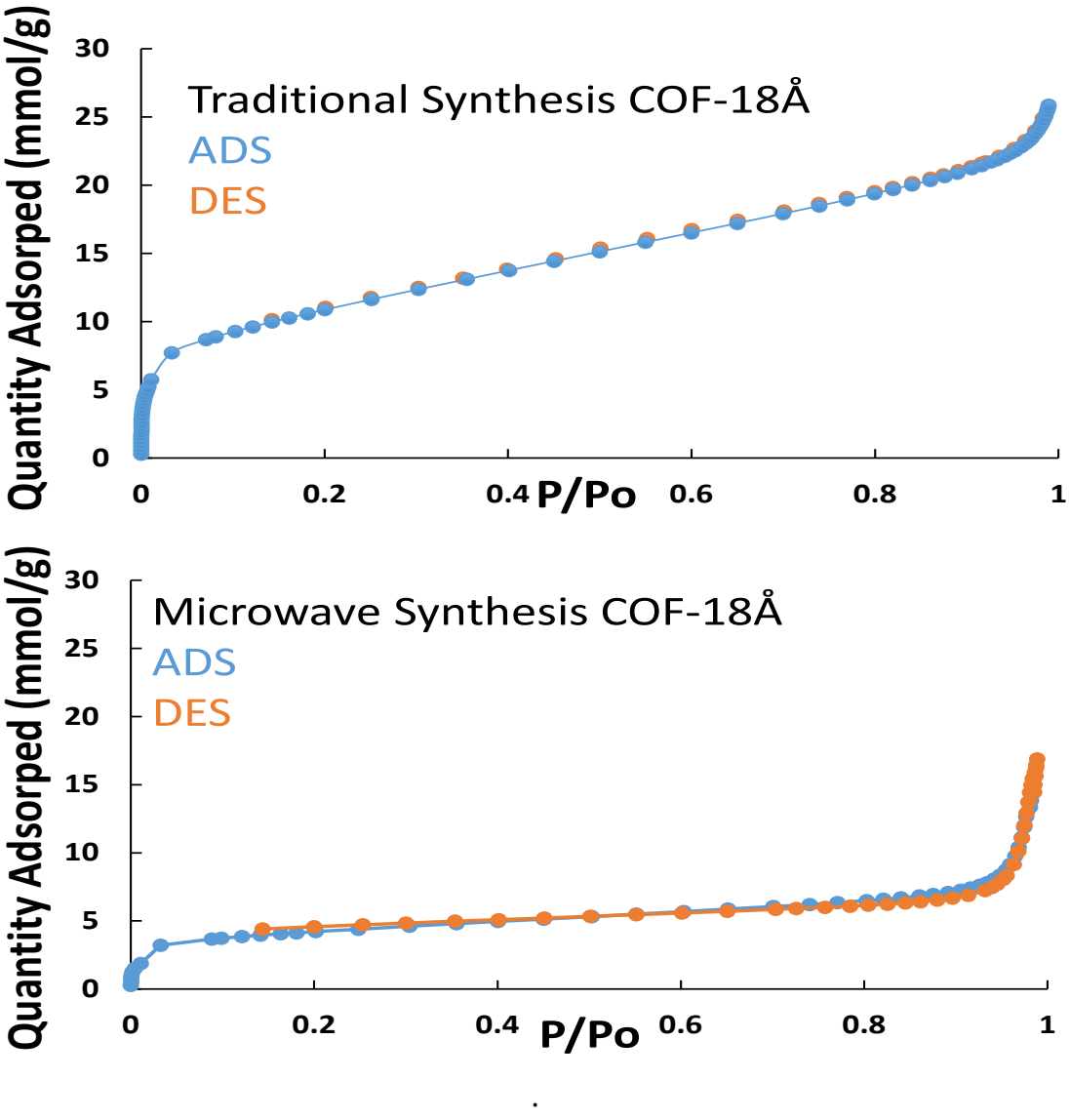

.

Figure D.1
Adsorption and desorption isotherm(s) of COFs larger image

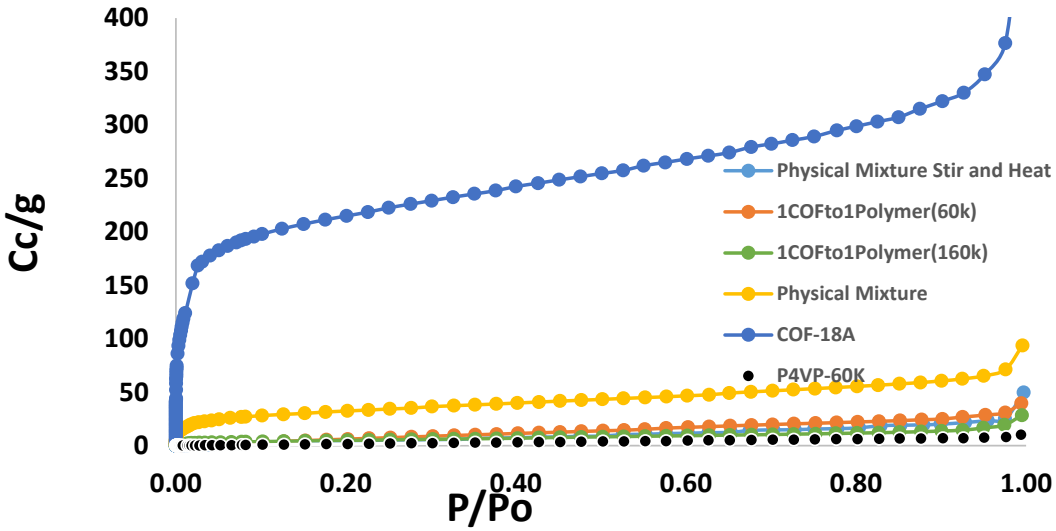

Figure D.2

Nitrogen Isotherms of physical mixture COFs

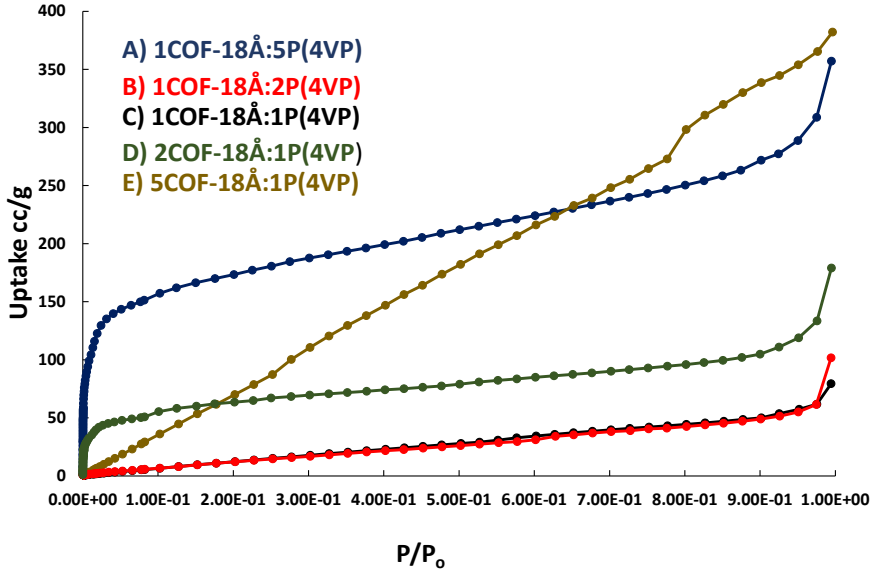

Figure D.3

Nitrogen Isotherms of Face Modified COFs various grafting densities.

Appendix E – UV-Vis

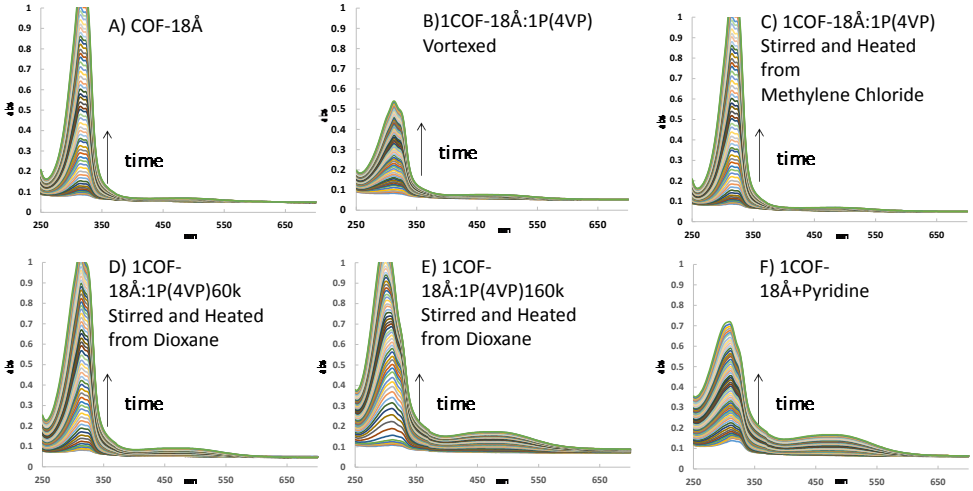

Figure E.1

UV Vis spectra of physical mixture COF.

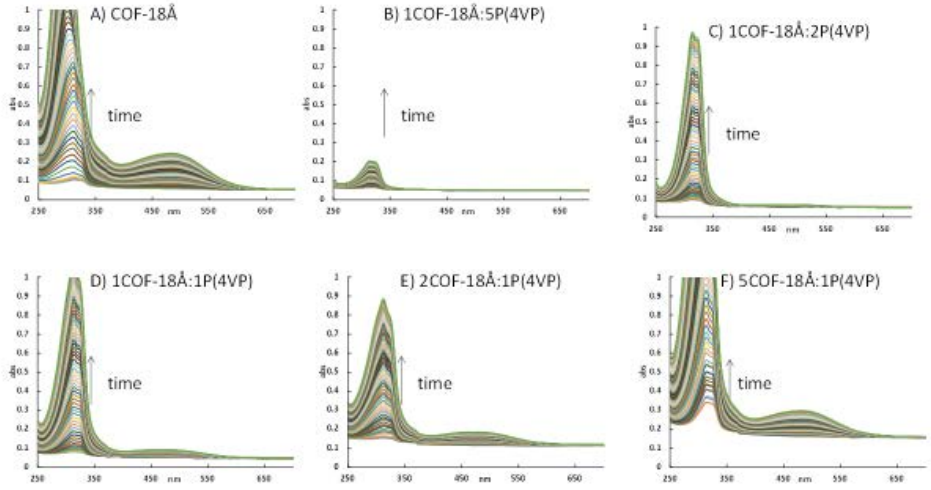

Figure E.2

UV Vis spectra of Face Modified COF various grafting densities.

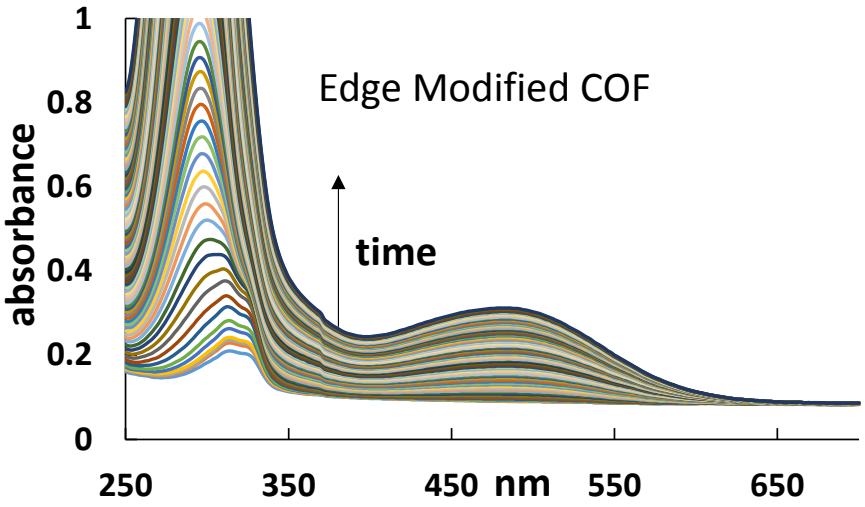

Figure E.3
UV Vis Spectra of Edge Modified COF.

Appendix F – Stability Studies

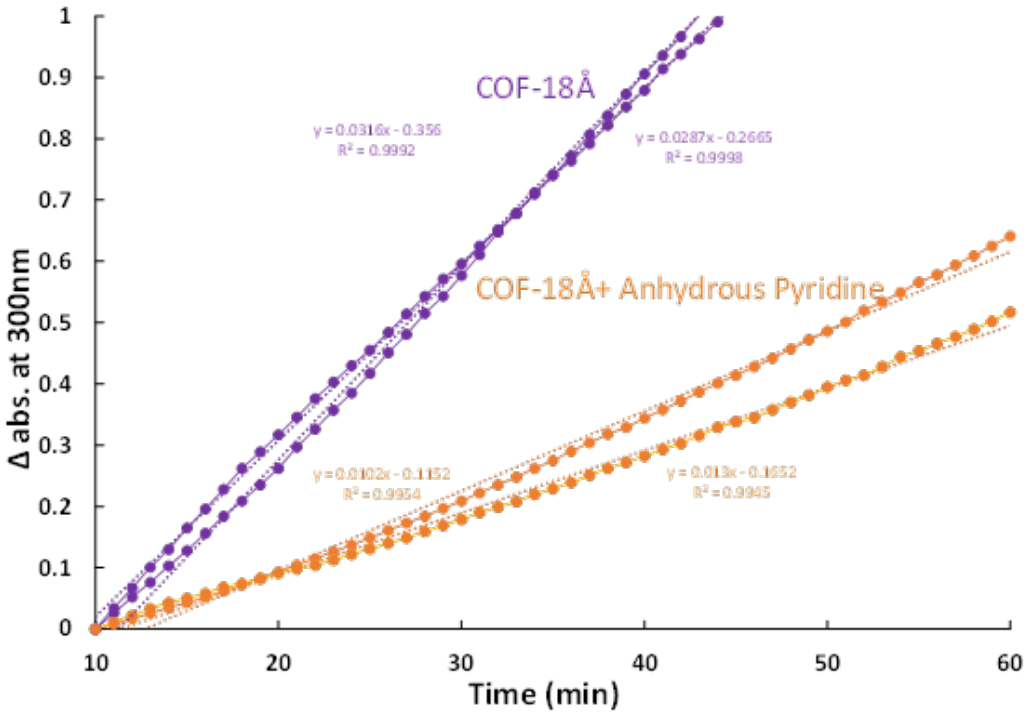

Figure F.1
Stability study of COF vs Face Modified COF.

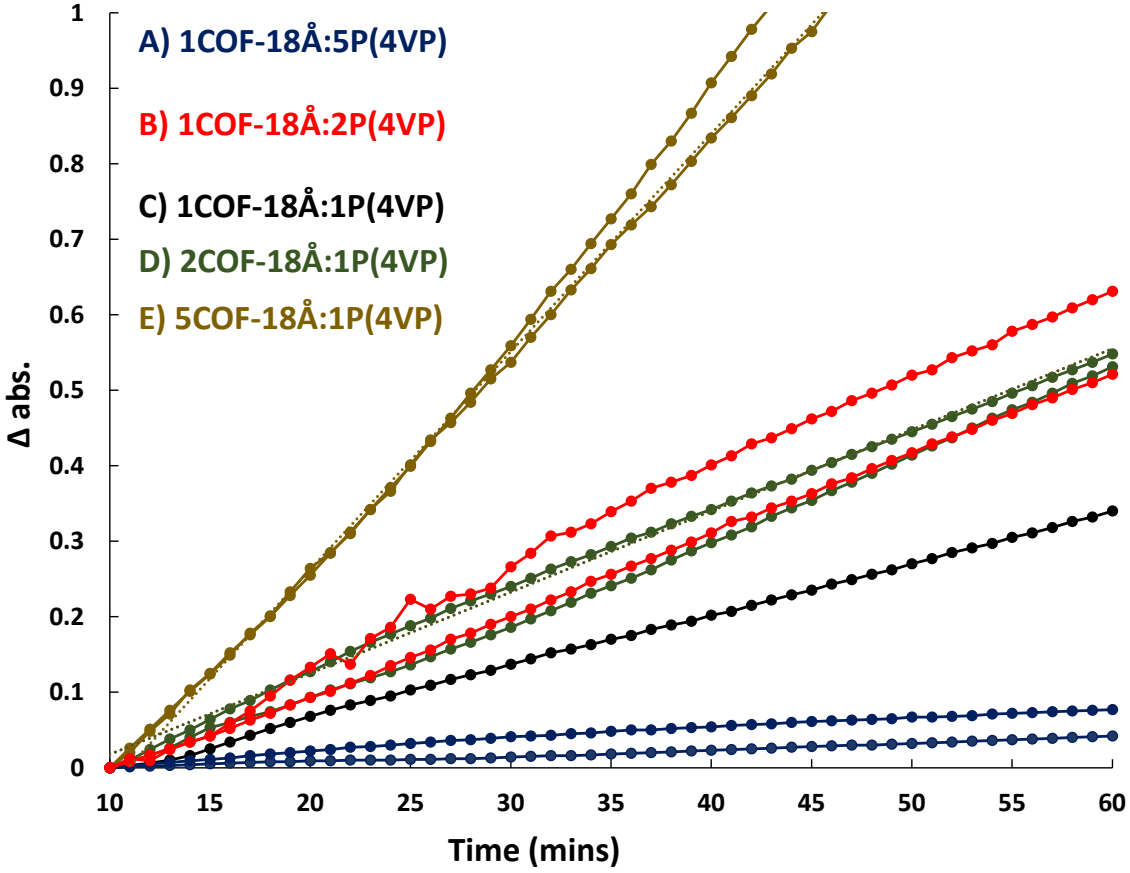

Figure F.2
Impact of grafting density on stability.

1

Appendix G – t-plots

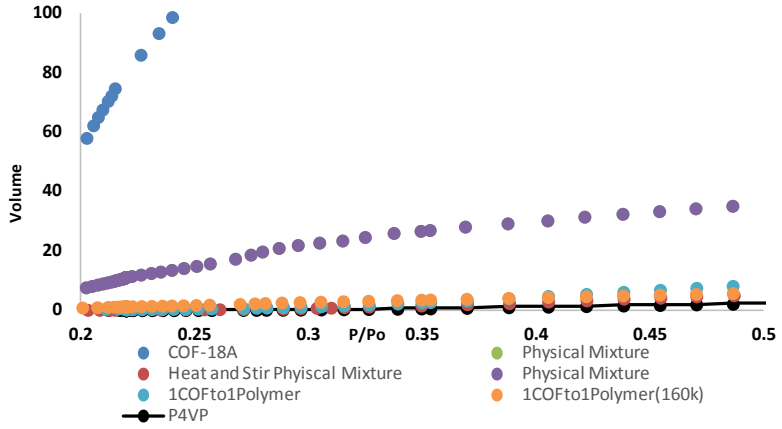

Figure G.1
t-Plot of physical mixture COFs.

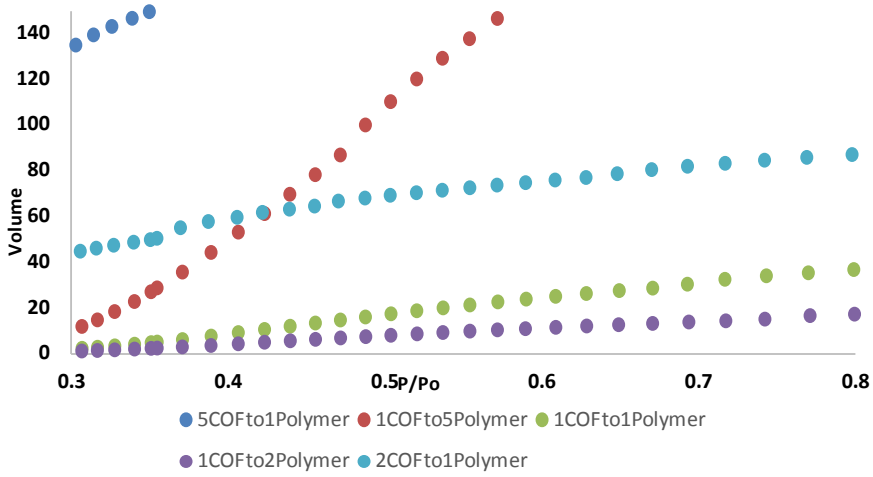

Figure G.2
t-Plot of various grafting density face modified COF.